Accepted Manuscript

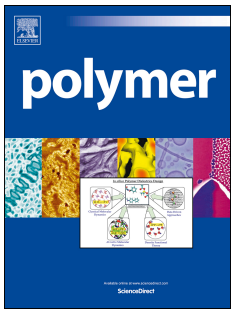

Water-Soluble Hyperbranched Poly(phenyleneethynylene)s: Facile Synthesis, Characterization, and Interactions with dsDNA

Yan-Qin Huang, Rui Zhang, Cai-Xia Song, Rong-Cui Jiang, Xing-Fen Liu, Guang-Wei Zhang, Qu-Li Fan, Lian-Hui Wang, Wei Huang

PII: S0032-3861(15)00002-6

DOI: 10.1016/j.polymer.2014.12.068

Reference: JPOL 17527

To appear in: *Polymer*

Received Date: 11 September 2014

Revised Date: 27 November 2014

Accepted Date: 31 December 2014

Please cite this article as: Huang Y-Q, Zhang R, Song C-X, Jiang R-C, Liu X-F, Zhang G-W, Fan Q-L, Wang L-H, Huang W, Water-Soluble Hyperbranched Poly(phenyleneethynylene)s: Facile Synthesis, Characterization, and Interactions with dsDNA, *Polymer* (2015), doi: 10.1016/j.polymer.2014.12.068.

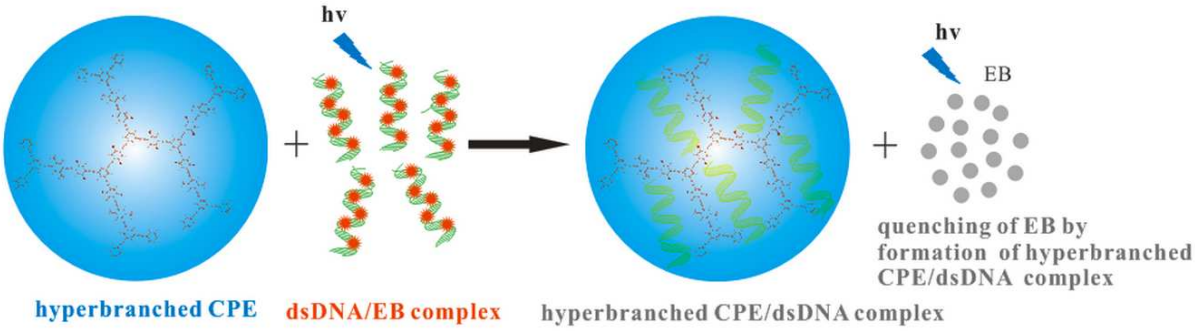

Water-Soluble Hyperbranched Poly(phenyleneethynylene)s: Facile Synthesis, Characterization, and Interactions with dsDNA

Yan-Qin Huang,[1,*] Rui Zhang,[3] Cai-Xia Song,[1] Rong-Cui Jiang,[1] Xing-Fen Liu,[1] Guang-Wei Zhang,[1] Qu-Li Fan,[1] Lian-Hui Wang,[1] Wei Huang[1, 2,*]

(1. Key Laboratory for Organic Electronics and Information Displays & Institute of Advanced Materials(IAM), Jiangsu National Synergistic Innovation Center for Advanced Materials (SICAM), Nanjing University of Posts & Telecommunications, 9 Wenyuan Road, Nanjing 210023, China.

2. Key Laboratory of Flexible Electronics (KLOFE) & Institute of Advanced Materials (IAM), Jiangsu National Synergistic Innovation Center for Advanced Materials (SICAM), Nanjing Tech University (NanjingTech), 30 South Puzhu Road, Nanjing 211816, China.

3. Department of Ophthalmology, Zhongda Hospital, Southeast University, Nanjing 211189, China.)

* To whom correspondence should be addressed: E-mail: iamyqhuang@njupt.edu.cn, Tel +86 25 8586 6396, Fax +86 25 8586 6396; E-mail: wei-huang@njtech.edu.cn, Fax: +86 25 5813 9988; Tel: +86 25 5813 9001.

Abstract

Two novel water-soluble hyperbranched poly(p-phenyleneethynylene)s (HBP1' and HBP2') bearing different contents of oligo(ethylene oxide) (OEO) side chains with ammonium end groups were synthesized by the facile "A_2 + B_2 (or A_2') + C_3" protocol based on Sonogashira polymerization. Their linear analogue (LP2') was also synthesized for comparative investigation. The optical properties of the neutral precursory polymers in THF and final cationic conjugated polyelectrolytes (CCPs) in aqueous solution were studied. Compared with LP2', HBP1' exhibited increased water solubility and fluorescence quantum yield despite its lower charge density, and HBP2', with the similar charge density as LP2', showed the best water solubility and the highest fluorescence quantum yield among the three CCPs. This indicated that the introduction of hyperbranched structure into conjugated polyelectrolytes was an efficient way to improve water solubility and fluorescence quantum yield because intermolecular aggregation was remarkably prevented. The interactions among the three CCPs and double-stranded DNA (dsDNA) were studied using ethidium bromide (EB) as the fluorescent probe. The electrostatic bindings of the three CCPs with dsDNA/EB complex resulted in displacement of EB from dsDNA to the solution accompanied by the quenching of EB fluorescence. Both HBP1' and HBP2' bound to dsDNA more efficiently than LP2', and HBP2' formed the most stable complex with dsDNA, suggesting that dsDNA might enter the cavities of single-molecular globular architectures of these hyperbranched conjugated polyelectrolytes and induced additional host-guest spatial interactions. Hence, HBP1' and HBP2' may be proved

very useful in gene delivery or DNA biosensor applications.

Keywords: Hyperbranched conjugated polyelectrolytes; Fluorescence; dsDNA

1. Introduction

Conjugated polyelectrolytes (CPEs) are synthetic macromolecules with highly delocalized π-conjugated backbones and hydrophilic polar side chains, which endow them with optoelectronic advantages of traditional conjugated polymers as well as water solubility and ionic nature of polyelectrolytes[1-3]. Amphiphilic CPEs can form complexes with acceptors (e.g., oppositely charged species, biological molecules) through noncovalent interactions, mainly including electrostatic interactions, hydrophobic interactions and π-π aromatic interactions. Thus, excitons can efficiently transfer to lower electron/energy acceptor sites along long conjugated parts to superquench the fluorescence of CPEs or to amplify the signals of acceptors [1-3]. Over the past decade, these advantages have resulted in the wide exploration of CPEs as promising biosensor platform [1-10]. Beyond sensing, new functions of CPEs have also been recently achieved in biological imaging and biomedical applications, including gene delivery, drug delivery and release, etc. [11-16].

Although CPEs have been proven useful in these applications, most of them reported in the literature have linear backbone structures and thus are “rigid-rod” like molecules [1-3]. Such molecular configuration cannot adapt to the range of secondary structures presented by biological macromolecules [17]. In aqueous media, the intermolecular interactions of CPEs with linear backbones result in tight aggregates, which may not only lead to fluorescence quenching due to π-stacking between the backbones of CPEs, but also reduce spatial interactions with biological macromolecules [17-19]. Therefore, the efficiencies of linear CPEs in their

applications above would be weakened. As promising materials, hyperbranched CPEs have been anticipated to overcome these drawbacks of linear CPEs [20-25].

Hyperbranched polymers are intriguing highly branched macromolecules with three-dimensional dendritic architectures [26-28]. In contrast with multigenerational dendritic polymers which require stepwise synthesis with complicated purification processes, hyperbranched polymers are easier to be synthesized in a one-pot procedure as well as show comparable properties [25]. We have employed the steric repulsions induced by highly branched and globular molecular structures of hyperbranched polymers to prevent the strong aggregation of linear conjugated polymers (CPs), and thus have developed some stable and strong blue light emitting CPs [29]. Furthermore, as the water-soluble derivatives of hyperbranched CPs, amphiphilic hyperbranched CPEs can exhibit single-molecular globular architectures with many cavities in aqueous media, and the functional groups on hydrophilic side chains extending into the aqueous solvent can provide binding forces for bioconjugation [20,24,25]. Such molecular configuration can be expected to improve contacts and binding stability between the molecules of hyperbranched CPEs and biological macromolecules as compared with the aggregate structure of linear CPEs.

Double-stranded DNA (dsDNA) with high density of negatively charged phosphate has been demonstrated in the studies of gene delivery to form rather stable complexes with polycations through electrostatic interactions [30,31]. Binding stability of these complexes is one of the chief requirements in the applications of gene delivery. Based on this point, some dendronized conjugated polyelectrolytes

with cationic charges have been developed for studying gene delivery [32]. Publications introducing the studies of hyperbranched CPEs in gene delivery have been very limited to date [33]. Herein, we designed and synthesized two structurally analogous hyperbranched water-soluble poly(phenyleneethynylene)s (PPEs) with different cationic charge densities through a simple "A_2 + B_2 (or A_2') + C_3" protocol based on Sonogashira polymerization. Water-soluble PPEs were used here because they show good optical responses to environmental variations and are suitable for studying structure–property relationships [34-37]. We successfully modulated their charge densities by adjusting the content of hydrophilic oligo(ethylene oxide) (OEO) side chain with ammonium end group. Meanwhile, the linear analogue of these hyperbranched CPEs was also synthesized to study the influence of molecular configuration on their properties, including optical properties and their interactions with dsDNA. The studies on the complex formations of these cationic conjugated polyelectrolytes (CCPs) with dsDNA indicated that the hyperbranched CPE with higher cationic charge density on the side chains formed the most stable complex with dsDNA.

2. Experimental Section

2.1. Materials

Toluene was purified by distillation from sodium in the presence of benzophenone. Ethidium bromide (EB) was purchased from Shanghai Genebase Gene-Tech Co., Ltd. (China). All other chemical reagents were purchased from either J&K Scientific Ltd. (Shanghai, China) or Sinopharm Chemical Reagent Co., Ltd (Shanghai, China), and

used without further purification. All oligonucleotides were purchased from Shanghai Sangon Biological Engineering Technology & Service Co., Ltd. (China). All aqueous solutions were prepared with MilliQ water (18.2 MQ cm) from a Millipore system. 1, 2-Bis(2-bromoethoxy)ethane [38], 1,4-dibromo-2,5-hydroquinone [39] and 1,4-diethynylbenzene (Monomer B_2) [40] were synthesized according to the literature procedures.

2.2. General Methods

NMR spectra were collected on a Bruker Ultra shield Plus 400 spectrometer with tetramethylsilane as the internal standard. UV-Vis spectra were recorded on a Shimadzu 3600 PC spectrophotometer. Photoluminescence (PL) measurement was carried out on a Shimadzu RF-5301 PC spectrofluorophotometer with a xenon lamp as a light source. Mass spectra were recorded on a Shimadzu GCMS-QP2010 plus equipped with DB-5 ms column. Elemental microanalyses were carried out on a Vario EL III CHNOS Elemental Analyzer. Molecular weight measurements were performed by Shimadzu Shim-pack GPC-800 gel permeation chromatography with polystyrenes as the standard and tetrahydrofuran (THF) as the eluant.

The optical properties of polymers were studied in dilute solutions (c = 1 μM, based on polymer repeat unit). All fluorescence spectra were recorded in a 3 mL quartz cuvette with an optical path length of 1.0 cm. Milli-Q water used in preparing the aqueous solutions of the polymers and quenchers was purged with nitrogen for 4 h before using. DNA concentrations were determined by measuring the UV-vis absorbance at 260 nm in 3 mL quartz cuvettes. The double-stranded DNA (dsDNA)

was obtained by annealing the mixtures of complementary strands in a buffer solution (10 mM tris-HCl, 100 mM NaCl, pH 7.5) at 2°C below the melting temperature T_m for 20 min and then slowly cooled to room temperature.

2.3. Synthesis of 1,4-Bis(2-(2-(2-bromoethoxy)ethoxy)ethoxy)-2,5-dibromobenzene (Compound 1)

A 100 mL round-bottom flask with magnetic stirring bar was charged with anhydrous potassium carbonate (8 g, 57.3 mmol), 1,4-dibromo-2,5-hydroquinone (2.56 g, 9.52 mmol), and 25 mL of acetonitrile. When the temperature of the mixture reached 70 °C, 1, 2-bis(2-bromoethoxy)ethane (26.27g, 95.2 mmol) was added into the flask, then the reaction mixture was stirred at this temperature for 24 h. After it was cooled to room temperature, the mixture was poured into a large volume of water and extracted with dichloromethane. The organic phase was dried over anhydrous sodium sulfate, filtered and stripped of solvent by rotary evaporation. The residue was purified by silica gel column chromatography (petroleum ether/ethyl acetate = 5:1) to give a white solid (3.2 g, yield: 50.5 %). Mp: 46-48℃. ^{1}H NMR (400 MHz, $CDCl_3$): δ (ppm) 7.16 (s, 2H), 4.13 (t, J = 6.5 Hz, 4H), 3.86–3.91 (m, 4H), 3.83 (t, J = 6.3 Hz, 4H), 3.77–3.79 (q, 4H), 3.69–3.72 (q, 4H), 3.48 (t, J = 6.3 Hz, 4H). Anal. Calcd for $C_{18}H_{26}Br_4O_6$: C, 32.86; H, 3.98. Found: C, 32.82; H, 3.96.

2.4. Synthesis of 1,4-Bis(2-(2-(2-N,N-diethylaminoethoxy)ethoxy)ethoxy)-2,5-dibromobenzene (Monomer A_2)

Compound 1 (0.8 g，1.2 mmol) was dissolved in 20 mL boiling diethylamine and

the reaction mixture was refluxed for 10 h. After the removal of excess diethylamine, water was added to dissolve the precipitate and then extracted with ether for three times. The combined organic layer was dried over anhydrous sodium sulfate. After removing the solvent, the residue was purified by silica gel column chromatography (petroleum ether/ethyl acetate/triethylamine = 75:25:3) to give a yellow oil (0.68 g, yield: 87.2%). ^{1}H NMR (400 MHz, $CDCl_3$): δ (ppm) 7.14 (s, 2H), 4.13 (t, J = 6.5 Hz, 4H), 3.84 –3.92 (m, 4H), 3.73–3.79 (m, 4H), 3.61–3.67 (m, 4H), 3.57 (t, J = 6.5 Hz, 4H), 2.67 (q, J = 6.7 Hz, 4H), 2.56 (q, J = 7.1 Hz, 8H), 1.02 (t, J = 7.0 Hz, 12H). ^{13}C NMR (100 MHz, $CDCl_3$): δ (ppm) 147.5, 120.4, 110.8, 70.5, 70.2, 70.0, 69.8, 68.7, 50.9, 49.9, 13.3. Anal. Calcd for $C_{26}H_{46}Br_2N_2O_6$: C, 48.61; H, 7.22; N, 4.36. Found: C, 48.58; H, 7.20; N, 4.33.

2.5. Synthesis of 1,4-Bis[(trimethylsilyl)ethynyl]-2,5-[bis(2-(2-(2-N,N-diethylaminoethoxy)ethoxy) ethoxy) benzene (Compound 2)

Under nitrogen protection, $Pd(PPh_3)_2Cl_2$ (49.2 mg，0.07 mmol), and CuI (26.8 mg，0.14 mmol) were added to a solution of Monomer A_2 (1.5 g，2.336 mmol) in 15 mL of diisopropylamine. Trimethylsilyl acetylene (0.46 g, 4.7 mmol) was slowly added to the mixture at room temperature. The reaction mixture was then refluxed under nitrogen for 6 h. The solvent was stripped off under reduced pressure. The residue was passed through a short column of silica gel using petroleum ether/ethyl acetate/triethylamine (75:25:3) as the eluent. Evaporation of the solvent led to a yellow oil (0.866 g, yield: 61%). ^{1}H NMR (400 MHz, $CDCl_3$): δ (ppm) 6.90 (s, 2H),

4.13 (t, J = 6.5 Hz, 4H), 3.85–3.93 (m, 4H), 3.77–3.79 (m, 8H), 3.61–3.63 (m, 4H), 3.55 (t, J = 6.5 Hz, 4H), 2.65 (q, J = 6.7 Hz, 4H), 2.55 (q, J = 7.1 Hz, 8H), 1.01 (t, J = 7.0 Hz, 12H), 0.25 (s, 18H). Anal. Calcd for $C_{36}H_{64}N_2O_6Si_2$: C, 63.86; H, 9.53; N, 4.14. Found: C, 63.88; H, 9.52; N, 4.16

2.6. Synthesis of 1,4-Diethynyl-2,5-[bis(2-(2-(2-N,N-diethylaminoethoxy)ethoxy)ethoxy)benzene (Monomer A_2')

Methanol (5 mL) and aqueous potassium hydroxide (0.4 g, 20%) were added to a stirred solution of Compound 2 (0.8 g, 1.32 mmol) in THF (8 mL) at room temperature. After the reactant was stirred at room temperature for 1 h, a large volume of water was poured into it, and then the mixture was extracted with dichloromethane. The extract was washed with water for three times, with brine once, and then dried over anhydrous sodium sulfate. After the solvent was removed, the residue was passed through a short column of silica gel using petroleum ether/ethyl acetate/triethylamine (60:30:2) as the eluent. Evaporation of the solvent led to a yellow oil (0.51 g，yield：72 %). ^{1}H NMR (400 MHz, $CDCl_3$): δ (ppm) 6.99 (s, 2H), 4.14 (t, J = 6.5 Hz, 4H), 3.85-3.88 (m, 4H), 3.73-3.76 (m, 4H), 3.61-3.63 (m, 4H), 3.54-3.57 (t, J = 6.5 Hz, 4H), 3.34 (s, 2H), 2.65 (q, J = 6.7 Hz, 4H), 2.55 (q, J = 7.1 Hz, 8H), 1.01 (t, J = 7.0 Hz, 12H). ^{13}C NMR (100 MHz, $CDCl_3$): δ (ppm) 151.4, 118.4, 112.3, 82.4, 81.5, 70.5, 70.2, 70.0, 69.9, 68.7, 50.8, 49.9, 13.2. Anal. Calcd for $C_{30}H_{48}N_2O_6$： C, 67.64; H, 9.08; N, 5.26. Found: C, 67.68; H, 9.04; N, 5.23.

2.7. General procedures for the synthesis of linear neutral polymers LP1 and LP2

Under nitrogen protection, degassed diisopropylamine/toluene (1:2, 12 mL) was added to a 25 mL round-bottom flask containing 0.128 g (0.2 mmol) of Monomer A_2 and 0.22 mmol diethynylbenzene monomer (0.028 g Monomer B_2, or 0.117 g of Monomer A_2'), 6 mg (0.005 mmol) of $Pd(PPh_3)_4$, and 2 mg (0.01 mmol) of CuI. After the reaction mixture was stirred at 75 °C for 24 h, bromobenzene (0.1 g, 0.5 mmol) was added for end-capping the polymer for an additional 2 h. Upon cooling to room temperature, the reaction mixture was subjected to a $CHCl_3/H_2O$ workup. The organic phase was washed with water for three times, and then dried over anhydrous sodium sulfate. After the solution was concentrated, it was dropped into hexane (200 mL). The precipitate was filtered, dissolved in chloroform, and reprecipitated in hexane twice to obtain a yellow fibrous solid.

LP1：0.085 g (yield 70 %).^{1}H NMR (400 MHz, $CDCl_3$): δ (ppm) 7.56–7.44 (m, ArH), 7.05 (m, 2H), 4.11–4.27 (m, 4H), 3.45–3.90 (m, 16H), 2.55–2.90 (m, 12H), 1.05 (m, 12H). ^{13}C NMR (100 MHz, $CDCl_3$): δ (ppm) 151.3, 118.4, 112.5, 131.9, 122.5, 95.9, 84.3, 70.6, 70.3, 70.0, 69.8, 68.8, 50.9, 49.7, 13.3.

LP2：0.151 g (yield 74 %). ^{1}H NMR (400 MHz, $CDCl_3$): δ (ppm) 7.03 (m, ArH), 4.11–4.27 (m, 4H), 3.45–3.95 (m, 16H), 2.5–2.90 (m, 12H), 1.06 (m, 12H). ^{13}C NMR (100 MHz, $CDCl_3$): δ (ppm) 151.6, 118.6, 112.4, 84.4, 70.8, 70.4, 70.1, 69.9, 68.9, 50.8, 49.8, 13.2.

2.8. General procedures for the synthesis of hyperbranched neutral polymers HBP1 and HBP2

Under nitrogen protection, degassed diisopropylamine/toluene (1:2, 12 mL) was

added to a 25 mL round-bottom flask containing 0.128 g (0.2 mmol) of Monomer A_2, 0.22 mmol diethynylbenzene monomer (0.028 g Monomer B_2, or 0.117 g of Monomer A_2'), and Monomer C_3(4 mg，0.0126 mmol), 6 mg (0.005 mmol) of $Pd(PPh_3)_4$, and 2 mg (0.01 mmol) of CuI. After the reaction mixture was stirred at 75 °C for 48 h, bromobenzene (0.1 g, 0.5 mmol) was added for end-capping the polymer for an additional 2 h. The following procedures were the same as those of the linear neutral polymers. The products were both brown fibrous solid.

HBP1：0.066 g (yield 54%). ^{1}H NMR (400 MHz, $CDCl_3$): δ (ppm) 7.6–7.69 (m, ArH), 7.38–7.58 (m, ArH), 7.0–7.18 (m, ArH), 4.11–4.27 (m, 4H), 3.25–3.90 (m, 16H), 2.55–2.90 (m, 12H), 1.08 (m, 12H). ^{13}C NMR (100 MHz, $CDCl_3$): δ (ppm) 151.7, 135.8, 131.9, 122.4, 121.8, 118.5, 112.3, 95.9, 84.2, 70.7, 70.4, 70.1, 69.9, 68.8, 50.7, 49.9, 13.2.

HBP2：0.124 g (yield 61%). ^{1}H NMR (400 MHz, $CDCl_3$): δ (ppm) 7.5–7.65 (m, ArH), 6.97–7.15 (m, ArH), 4.11–4.29 (m, 4H), 3.45–3.95 (m, 16H), 2.45–2.90 (m, 12H), 1.08 (m, 12H). ^{13}C NMR (100 MHz, $CDCl_3$): δ (ppm) 151.7, 135.9, 121.9, 118.6, 112.5, 93.4, 84.3, 70.7, 70.3, 70.0, 69.7, 68.8, 50.7, 49.8, 13.3.

2.9. General procedure for the synthesis of cationic conjugated polyelectrolytes (CCPs) via quaternization of the neutral polymers

Ethyl bromide (6 mL) was added to 0.1 mmol of the neutral polymers dissolved in 10 mL THF at room temperature. After 10 min stirring, some precipitate was observed, which was redissolved by addition of 1 mL H_2O. After 5 days, the reaction mixture was concentrated and then poured into acetone to form a precipitate. After

stirring for two hours, the collected precipitate was redissolved with methanol. The solution was concentrated and poured into acetone again, and the precipitate was collected and dried at room temperature in vacuo to yield the target polymers.

LP2': 0.107 g (yield 74%). ^{1}H NMR (400 MHz, CD_3OD): δ (ppm) 7.1 (br, ArH), 4.14–4.30 (br, 4H), 3.5–3.95 (m, 16H), 2.55–3.0 (br, 12H), 1.15 (br, 12H). ^{13}C NMR (100 MHz, $CDCl_3$): δ (ppm) 151.6, 118.5, 112.4, 84.3, 70.7, 70.3, 70.0, 68.8, 68.2, 60.2, 55.4, 8.3.

HBP1': 0.065 g (yield 79%). ^{1}H NMR (400 MHz, CD_3OD): δ (ppm) 7.1–7.8 (m, ArH), 3.2–4.5 (m, 20H), 2.6–3.1 (m, 12H), 1.16 (br, 12H). ^{13}C NMR (100 MHz, $CDCl_3$): δ (ppm) 151.6, 135.8, 132.0, 122.5, 121.7, 118.6, 112.5, 95.8, 84.1, 70.7, 70.5, 70.2, 68.8, 68.2, 60.1, 55.5, 8.4.

HBP2': 0.12 g (yield 82%). ^{1}H NMR (400 MHz, CD_3OD): δ (ppm) 7.15–7.75 (m, ArH), 4.15–4.32 (br, 4H), 3.5–4.0 (m, 16H), 2.55–3.05 (br, 12H), 1.14 (br, 12H). ^{13}C NMR (100 MHz, $CDCl_3$): δ (ppm) 151.7, 135.8, 121.9, 118.5, 112.4, 93.3, 84.2, 70.6, 70.4, 70.1, 68.7, 68.1, 60.1, 55.4, 8.3.

3. Results and Discussion

3.1. Synthesis and characterization

The preparation of linear neutral polymers was accomplished via Sonogashira polymerization of Monomer A_2 and Monomer B_2 (or A_2') [34]. A simple ''A_2 + B_2 (or A_2') + C_3'' protocol based on Sonogashira polymerization was employed to synthesize the neutral hyperbranched polymers [22,29].

The synthetic routes for monomers A_2 and A_2' were shown in Scheme 1. In a basic

deprotonation condition, 1,4-dibromo-2,5-hydroquinone was alkylated with 1, 2-bis(2-bromoethoxy)ethane to afford Compound 1 [41,42], and then Monomer A_2 was synthesized by refluxing the mixture of Compound 1 and excess diethylamine [42]. Compound 2 was obtained via Sonogashira reaction of Monomer A_2 with trimethylsilyl acetylene, which was then stirred in the mixed solution of methanol and aqueous potassium hydroxide to produce Monomer A_2'. Monomer B_2 was prepared according to literature procedures [40]. The correct structures of Monomer A_2 , Monomer A_2' and Monomer B_2 were affirmed by ^{1}H NMR and ^{13}C NMR spectroscopy and elemental analysis.

Scheme 1. Synthetic routes for the monomers. Reagents and conditions: (a) 1, 2-bis(2-bromoethoxy)ethane, K_2CO_3, acetonitrile, 70 °C, 24 h; (b) $(C_2H_5)_2NH$, reflux, 10 h; (c) $(CH_3)_3SiCCH$, $(PPh_3)_2PdCl_2$, CuI, diisopropylamine, 6 h; (d) KOH, CH_3OH-THF, rt, 1 h.

Scheme 1

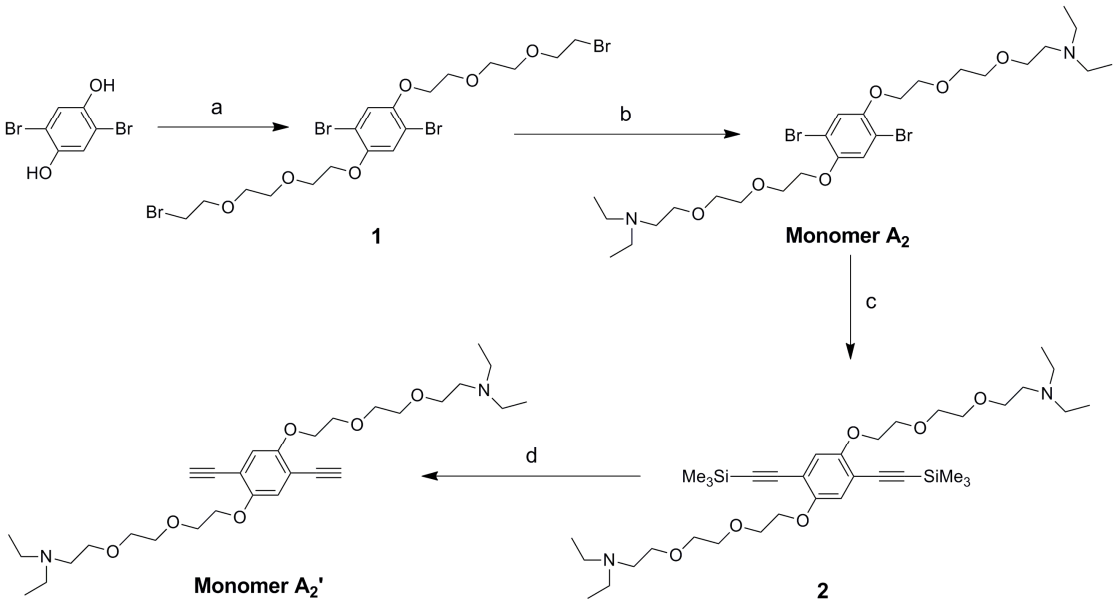

The synthetic routes for the polymers were illustrated in Scheme 2. GPC revealed that the four neutral polymers had close weight-average molecular weights (M_w)

ranging from 7250 to 7680 with the polydispersity indices in the range of 1.17–1.42 (Table 1). The solubility of the hyperbranched neutral polymers was dominantly determined by the molar ratio of the branching unit C_3. HBP1 and HBP2 with 3% C_3 (produced in the molar ratios of Monomer A_2:B_2(or A_2'):C_3) = 48:52:3) were fully soluble in common organic solvents, e.g., THF, chloroform, and CH_2Cl_2. Further increasing the contents of C_3 leads to a lower yield of soluble polymer due to crosslinking [22,29]. It was found that the solubility of the hyperbranched neutral polymers was obviously better than those of the linear neutral polymers. Moreover, LP1 showed poor solubility in THF and chloroform while LP2 showed better solubility than LP1 most likely due to the much higher density of side chains in LP2.

Table 1. Characterization of the Neutral Precursory Polymers and Cationic Conjugated Polyelectrolytes.

Entry	GPC			$\lambda_{abs,max}$ /nm		$\lambda_{em,max}$ /nm	
	M_n	M_w	PDI	THF	H_2O	THF	H_2O
LP1	5350	7600	1.42	395		451	
LP2	5450	7250	1.33	417		472	
HBP1	5870	7680	1.31	387		445	
HBP2	6360	7450	1.17	406		467	
LP2'					339		467
HBP1'					330		442
HBP2'					333		463

Scheme 2. Synthetic routes for the neutral and cationic polymers. Reagents and conditions: (a) $Pd(PPh_3)_4$, CuI, diisopropylamine/toluene, 75 °C, 24 h; (b) C_2H_5Br, THF-H_2O, 5 days; (c) $Pd(PPh_3)_4$, CuI, diisopropylamine/toluene, 75 °C, 48 h;

Scheme 2

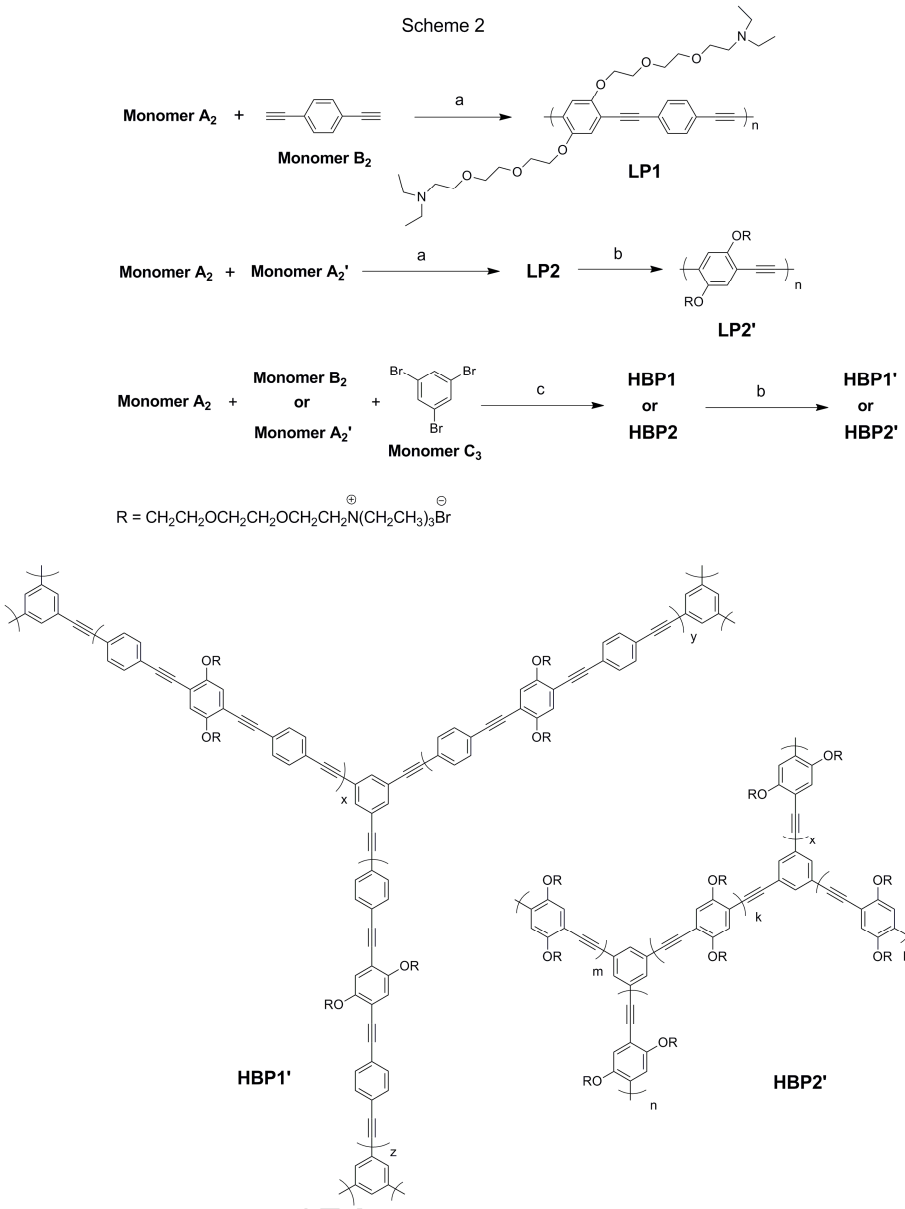

The structures of the polymers were characterized by ^{1}H NMR and ^{13}C NMR spectra. As shown in Fig. 1, all protons on the side chains of HBP1 and HBP2 could be well assigned, and the single peaks at δ =1.08 were assigned to the signals from –NCH$_2$***CH$_3$***– protons, evidently indicating the existence of the amine groups [36, 43]. Moreover, the characteristic proton signals of the branching units and phenylene units were observed at δ = 7.6–7.69, 7.38–7.58 and 7.0–7.18 ppm for HBP1, and at δ = 7.5–7.65 and 6.97–7.15 ppm for HBP2. Thus, the intergral ratios between the branching unit and phenylene of these two polymers can be approximately estimated

from ^{1}H NMR spectra, that is about 1:65 for HBP1 and 1:43 for HBP2, respectively, which can roughly reflect the relative amount of benzene unit [22,29]. The CCPs were synthesized through the postquaternization treatment of the neutral polymers with ethyl bromide in THF-H_2O solution [36]. However, the quaternization of LP1 was not achieved perhaps due to the poor solubility in THF. In the ^{1}H NMR spectra of the CCPs LP2', HBP1', and HBP2', nearly all signals moved to the lower field compared with those of LP2, HBP1, and HBP2, and there were no split peaks arising from the quaternized (low field) and unquaternized components, clearly indicating complete quaternization of these three neutral polymers [36,42,43]. The solubility for LP2', HBP1', and HBP2' in water (25 °C) was measured to be 8, 11 and 20 mg/mL, respectively. In view of the slight differences in the molecular weights of these WSCPs, it was rational to propose that the existence of hyperbranched structure as well as hydrophilic side chains would improve the water solubility of CPEs.

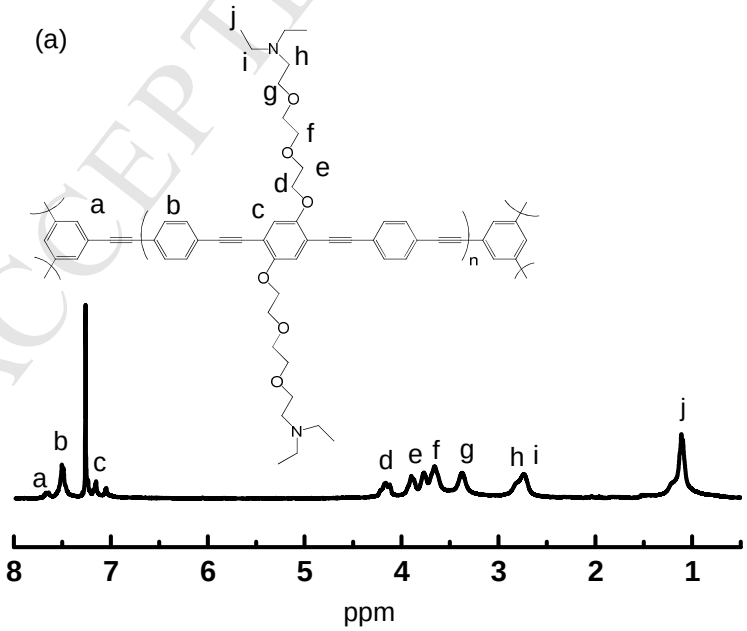

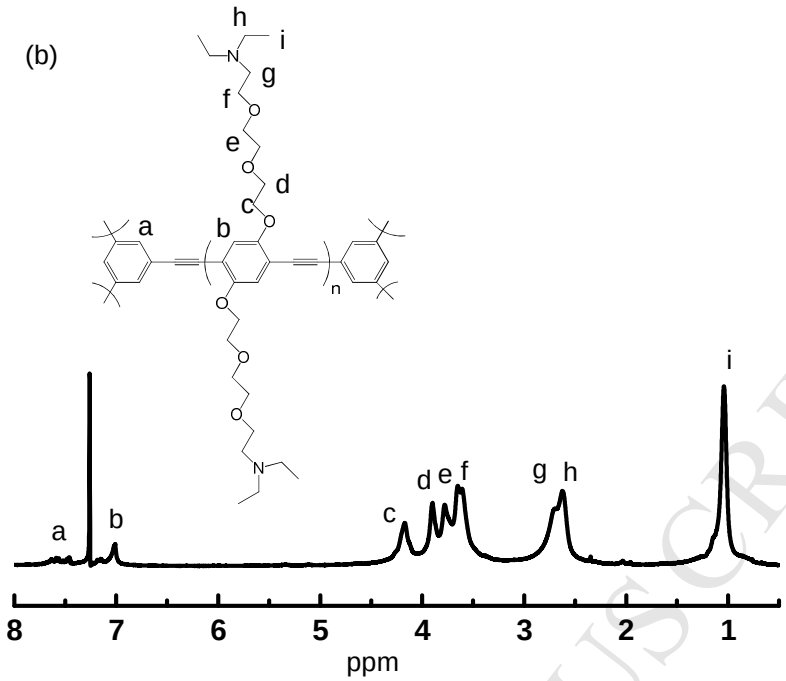

Fig. 1. ^{1}H NMR spectra of the hyperbranched neutral polymers (a) HBP1 and (b) HBP2.

3.2. Optical properties

The UV–vis absorption and PL spectra of the neutral precursory polymers in dilute THF solution resembled previously reported spectra of structurally analogous neutral PPEs (Fig. 2) [36]. The corresponding optical data were summarized in Table 1. The absorption and emission maxima of HBP1 were blueshifted 8 nm and 6 nm, respectively, as compared with the absorption and emission maximum of LP1. When comparing the optical data of HBP2 and LP2, we also found these similar phenomena. This can be attributed to the introduction of benzene branching unit in the structure of hyperbranched polymers, which interrupted the linear π-system and led to reduction in the effective conjugation length [22]. On the other hand, the absorption and emission maxima of HBP2 were redshifted 19 nm and 22 nm, respectively, as compared with the absorption and emission maximum of HBP1. These similar phenomena were also

observed while comparing the optical data of LP2 and LP1. In view of the higher density of side chains in the structure of HBP2 and LP2, these phenomena should be ascribed to the nonbonding electron pairs on the oxygen atoms of side chains, which contributed to the conjugation of the main chain and led to increase in the effective conjugation length [43,44].

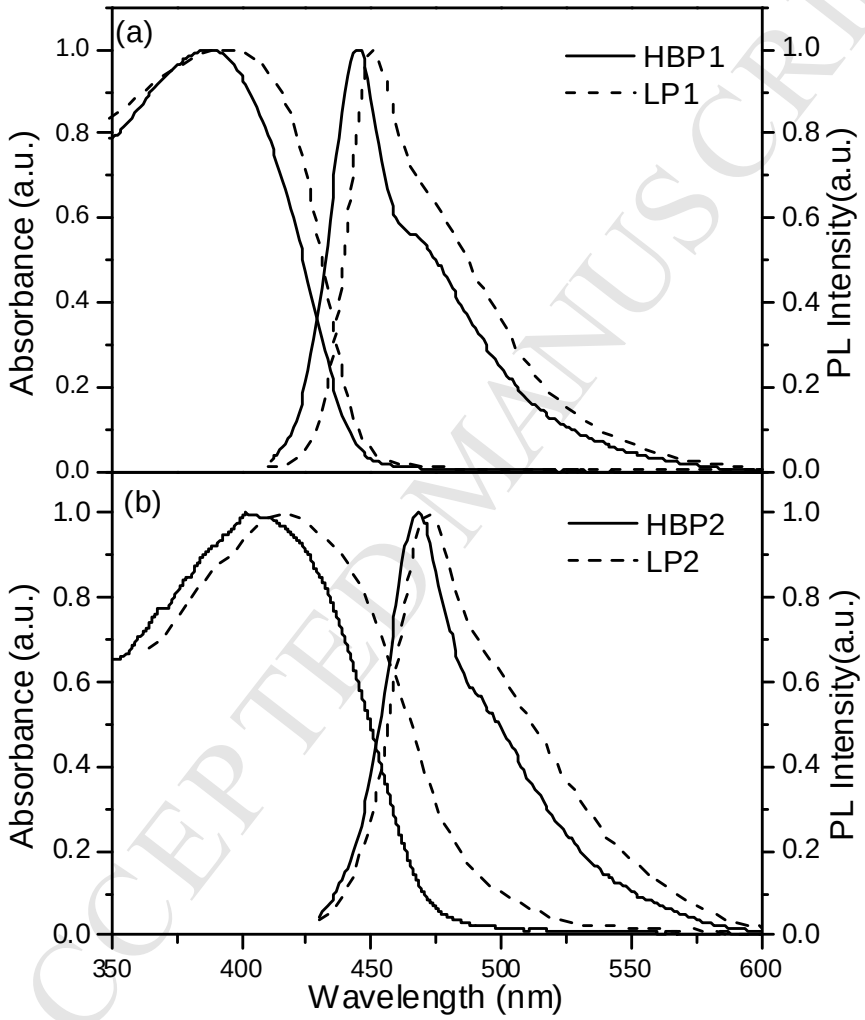

Fig. 2. UV–vis absorption and PL spectra of the neutral polymers (a) LP1 and HBP1, and (b) LP2 and HBP2 in THF.

The UV–vis absorption and PL spectra of LP2', HBP1' and HBP2' in water were shown in Fig. 3. In comparison with those of their neutral precursory polymers, the absorption and emission peaks of all quaternized polymers presented blue-shifts, and

the blue-shifts were especially obvious in the cases of absorption. This was likely due to the mutual repulsion among the positive charges, which resulted in a more twisted main chain conformation, hence a decreased effective conjugation length [36]. The fluorescence quantum yields (Φ_F) for LP2', HBP1' and HBP2' in water were measured to be 2.47%、2.7%、and 6.26%, respectively. HBP2' exhibited a much higher Φ_F than its linear analogue, LP2'. Moreover, although HBP1' had a lower density of hydrophilic side chains than LP2', it also presented a slightly higher Φ_F. Although the Φ_F of these PPEs were lower than those of the linear and hyperbranched polyfluorenes reported in a previous study, similar relationships between the structure and Φ_F have been found [22]. It was noted that Φ_F for the three CCPs followed the same order as their solubility in water. Therefore, it was rational to propose that the incorporation of hyperbranched structures into the CPEs can efficiently reduce the intermolecular aggregation, thus significantly improving the fluorescence efficiency as well as water solubility [20,22].

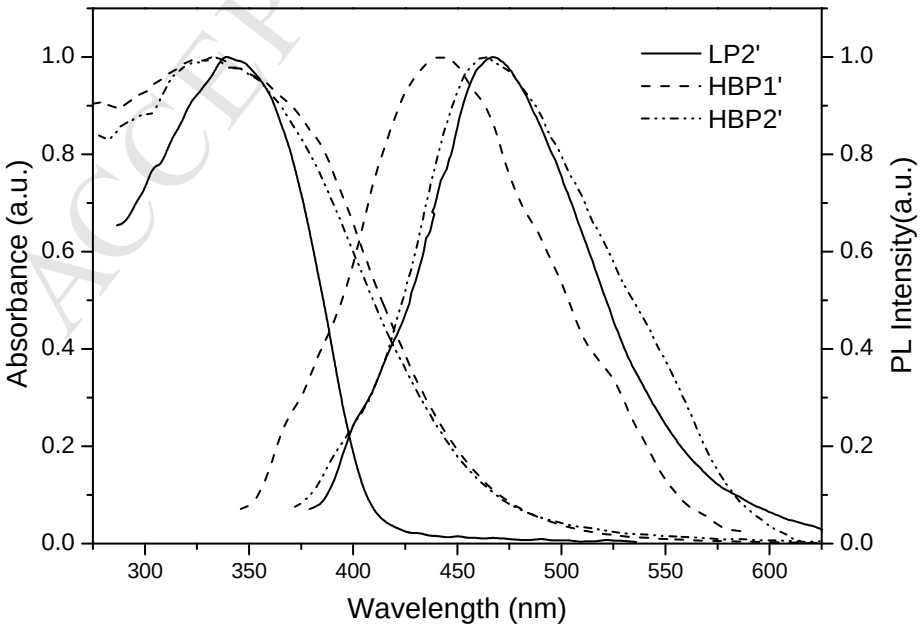

Fig. 3. UV–vis absorption and PL spectra of the CCPs LP2', HBP1', and HBP2' in water.

3.3. Interactions of the cationic conjugated polyelectrolytes with DNA

The interactions between dsDNA and the three CCPs were investigated by probing the PL intensity changes of the CCPs. The oligonucleotide used in these experiments was 5'-GAA CAT GGC AAG CTG-3'(ssDNA). The dsDNA was obtained by hybridization of the ssDNA with its complementary strand, 5'-CAG CTT GCC ATG TTC-3'($ssDNA_C$). As shown in Fig. 4(a), the maxima and shapes of the PL spectra of LP2' did not change and no new peaks appeared, and there was a substantial decrease in the emission of LP2' ([LP2'] = 1.0×10^{-6} M) upon adding dsDNA ([dsDNA] = 0 ~ 1.0×10^{-8} M) in the tris buffer solution (10 mM tris-HCl, 100 mM NaCl, pH = 7.5). The inset of Fig. 4(a) also exhibited that the PL intensity of LP2' obviously dropped after the interaction with dsDNA. It can be calculated from Fig. 4(b) that the PL intensity dropped about 27.5 percent as the concentration of dsDNA reached 1.0×10^{-8} M. The ammonium groups on the CCPs would be partially neutralized with the formation of CCP/dsDNA complex, leading to decreased charge density and thus a decrease in the intermolecular electrostatic repulsion. Therefore, LP2', with the planar and linear main chain of PPE [34-37], tended to form π-stacking aggregates near the negatively charged dsDNA, leading to self-quenching [32, 45, 46]. By contrast, such substantial quenching of emission was not found in the case of HBP2'. As shown in Fig. 4(c), the PL intensity dropped less than 7 percent as the concentration of dsDNA reached 1.0×10^{-8} M. Similar result was also obtained for HBP1'. These results can also be explained by the highly branched and rigid globular

molecular structures of HBP2' and HBP1', which efficiently reduce the intra- and intermolecular aggregation with the addition of dsDNA, thus significantly inhibiting self-quenching [22,32].

Figure 4(a)

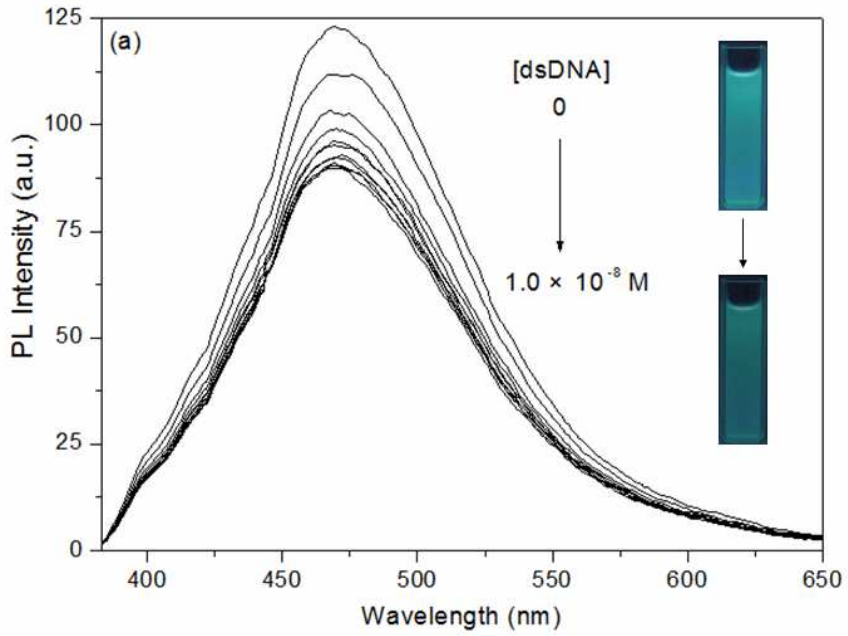

Figure 4(b)

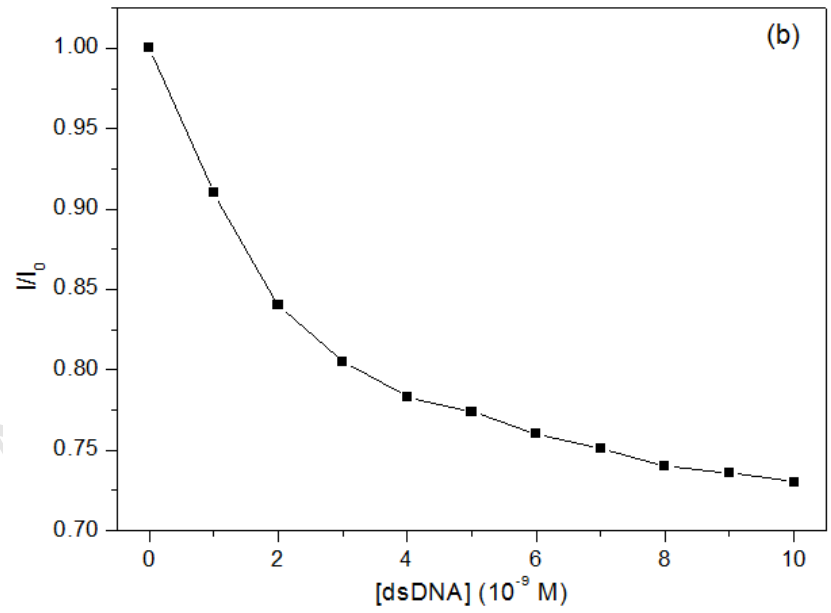

Figure 4(c)

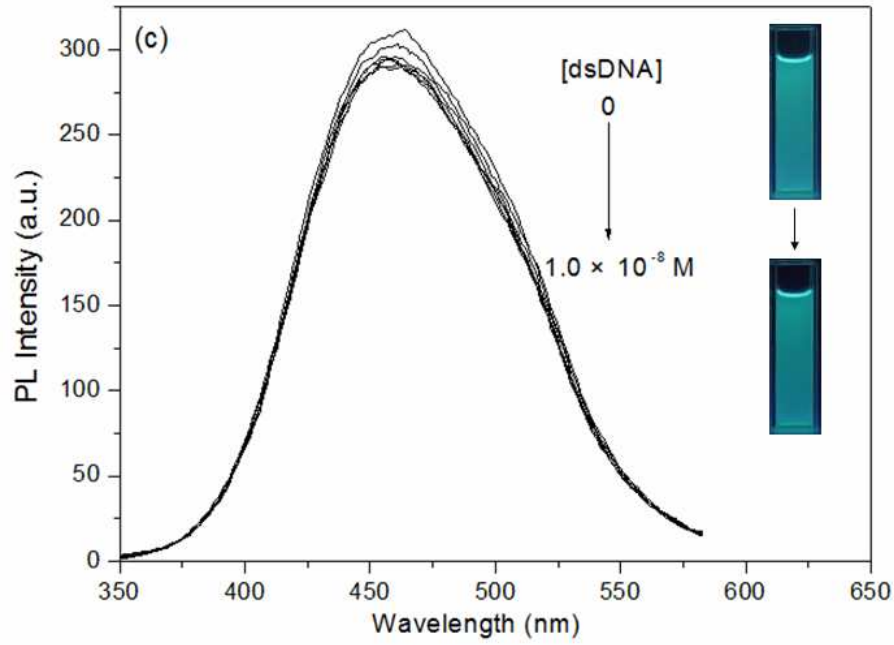

Fig. 4. (a) PL spectra of LP2' with the presence of dsDNA at different concentrations, [dsDNA] = 0 to 1.0×10^{-8} M, [LP2'] = 1.0×10^{-6} M, λ_{ex} = 339 nm. The inset shows the fluorescent photos of LP2'/dsDNA solutions when dsDNA concentration was 0 and 1.0×10^{-8} M, respectively. (b) Normalized PL intensity of LP2' as a function of dsDNA concentration. (c) PL spectra of HBP2' with the presence of dsDNA at different concentrations, [dsDNA] = 0 to 1.0×10^{-8} M, [HBP2'] = 1.0×10^{-6} M, λ_{ex} = 333 nm. The inset shows the fluorescent photos of HBP2'/dsDNA solutions when dsDNA concentration was 0 and 1.0×10^{-8} M, respectively. Measurements were performed in the tris buffer solution (10 mM tris-HCl, 100 mM NaCl, pH = 7.5). The fluorescent photos were taken under a portable UV lamp with excitation at 365 nm.

The interactions between dsDNA and the three CCPs were also investigated by using cationic ethidium bromide (EB) as a fluorescent probe. EB is a dsDNA-specific intercalator which shows an evident increase in fluorescence intensity upon intercalating into the double helix of dsDNA [47,48]. However, free EB exhibits a very low fluorescence intensity in buffer solution. Hence, the binding properties of other cationic species to dsDNA can be studied by using EB as competitor [32,49].

The electrostatic bindings of the three CCPs with dsDNA/EB complex would lead to displacement of intercalated EB from dsDNA to the solution due to the electrostatic repulsion, and this was accompanied by the quenching of EB fluorescence. Thus, the stability of the CCP/dsDNA complex can be evaluated by studying the fluorescence changes of EB. First, the dsDNA and EB were premixed in the tris buffer solution (10 mM tris-HCl, 100 mM NaCl， pH = 7.5) ([dsDNA] = 1.0×10^{-8} M, [EB] = 3.0×10^{-7} M), and the CCP was successively added to the solution ([HBP2'] = 0 to 1.0×10^{-7} M, [HBP1'] = [LP2'] = 0 to 1.0×10^{-6} M) followed by excitation at the absorption maximum of EB (480 nm). As shown in Fig. 5(a), the PL intensity of dsDNA/EB decreased gradually as the concentration of HBP2' increased. The decrease of PL intensity were also observed for HBP1' and LP2'. The normalized PL intensity of dsDNA/EB (I/I_0) as functions of the CCP concentrations were illustrated in Fig. 5(b, c). It was noted that the linear plots were obtained for both HBP2' and HBP1', whereas an upsloping nonlinear line was observed for LP2'. Moreover, the decline of I/I_0 upon adding HBP2' exhibited nearly ten times the rate of decline upon adding HBP1'. Interestingly, although the charge density of HBP1' was much lower than that of LP2', the value of I/I_0 with the addition of HBP1' decreased more greatly than with the addition of LP2'. Most importantly, as the stability of the CCP/dsDNA complex has close relationship with the ratio of positive charge to negative charge, we also studied the variation of I/I_o with molar ratio of amine (on LP2', HBP1' and HBP2') to phosphate (on dsDNA). The data in Fig. 5(d) showed similar trends to those in Fig. 5(b, c), namely, the rate of decline of I/I_0 also followed the order HBP2' >HBP1'>

LP2'. All these results indicated that the hyperbranched CPEs HBP2' and HBP1' bound to dsDNA more efficiently than their linear analogue LP2'.

Figure 5(a)

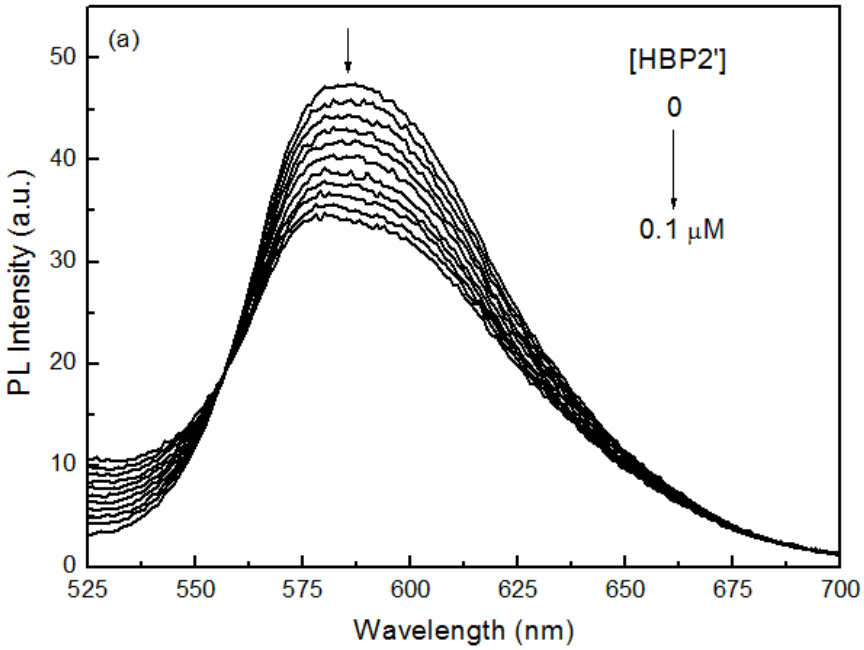

Figure 5(b)

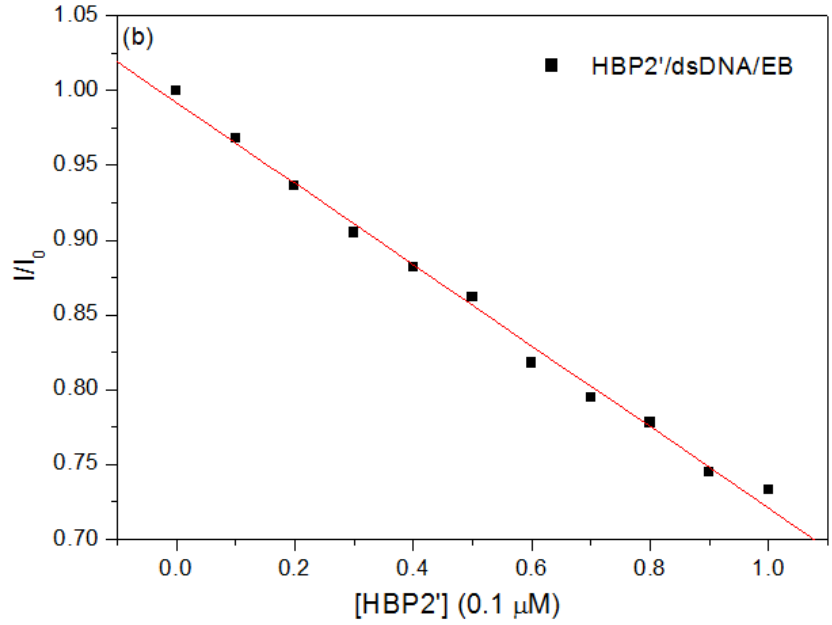

Figure 5(c)

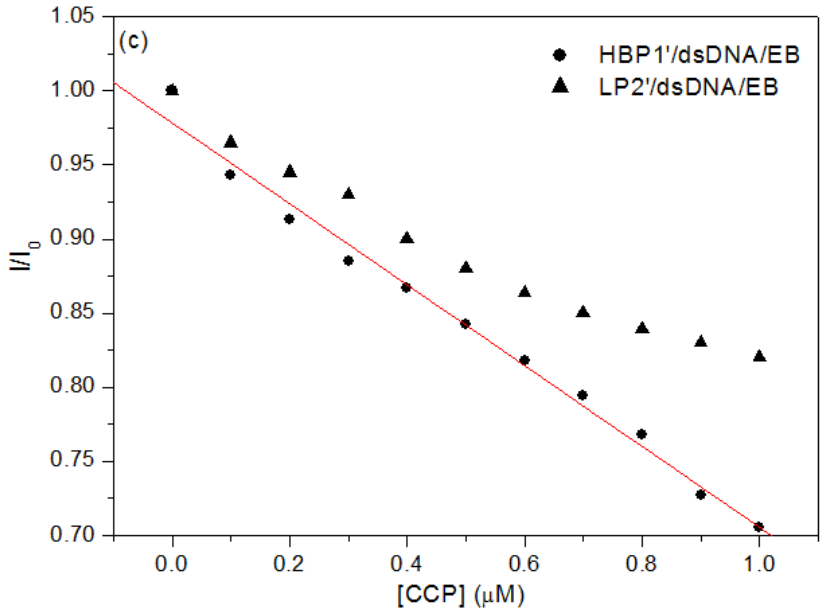

Figure 5(d)

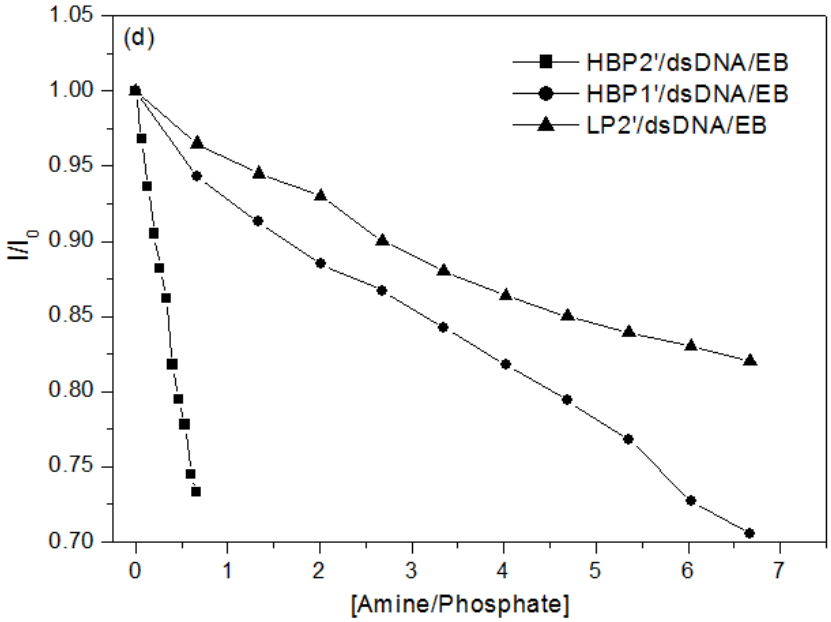

Fig. 5. (a) PL spectra of dsDNA/EB as a function of HBP2' concentration. (b) Normalized PL intensity of dsDNA/EB as a function of HBP2' concentration. (c) Normalized PL intensity of dsDNA/EB as functions of HBP1' and LP2' concentrations. (d) Normalized PL intensity of dsDNA/EB as functions of molar ratio of amine (on LP2', HBP1' and HBP2') to phosphate (on dsDNA). [dsDNA] = 1.0 × 10^{-8} M, [EB] = 3.0× 10^{-7} M, [HBP2'] = 0 to 1.0 × 10^{-7} M, [HBP1'] = [LP2'] = 0 to 1.0 × 10^{-6} M, λ_{ex} = 480 nm. Measurements were performed in the tris buffer solution (10

mM tris-HCl, 100 mM NaCl, pH = 7.5).

We compared these results with those in a previous literature which also studied the interactions between water-soluble conjugated polyfluorenes with dendritic side chains and dsDNA using EB as fluorescent probe [32]. Among three polymers with the same conjugated backbones, the polymer with highest generation of dendritic side chains, namely, highest charge density, was reported to form most stable complex with dsDNA [32]. However, in our cases, the charge density of HBP2' was close to that of LP2', and for HBP1', it was even lower than LP2'. Hence, in addition to the charge densities of the CCPs, the state of aggregation may be the other crucial factor that influenced the stability of the CCP/dsDNA complexes. As discussed above, compared with HBP2' and HBP1', LP2' exhibited a greater tendency to form π-stacking aggregates, which may make the polymer less accessible to dsDNA [43, 50], subsequently reduce the binding efficiency and lead to the upsloping nonlinear line in Fig. 5c. However, as for HBP2' and HBP1', the single-molecular globular architectures with many cavities and with cationic ammonium end groups on extending side chains, can not only effectively prevent the formation of intra- and intermolecular aggregates, but also may provide the advantages of more chances to contact dsDNA. According to previous literatures, these molecular configuration features of hyperbranched CPEs may make them useful host molecular carriers for organic molecules and biomacromolecules in applications [20,24,25]. Therfore, as shown in Scheme 3, we suggested that dsDNA might enter the cavities of highly branched structure as a guest molecule, which resulted in more spatial interactions

and thereby significantly improved the binding stability of hyperbranched CPE/dsDNA complex.

4. Conclusion

In summary, two structurally analogous water-soluble hyperbranched PPEs (HBP1' and HBP2') with different cationic charge densities were synthesized by the simple "A_2 + B_2 (or A_2') + C_3" protocol based on Sonogashira polymerization. Their linear analogue (LP2') was also synthesized for comparative investigation. The optical properties of these CCPs and their corresponding neutral polymers were studied by UV–vis and PL spectroscopy. All the three CCPs had good water solubility. In particular, HBP1' and HBP2' exhibited obviously increased water solubility and fluorescence quantum yield compared with that of their linear analogue LP2', indicating that the introduction of hyperbranched structures into CPEs is an efficient way to improve water solubility and fluorescence quantum yield. Moreover, among these CCPs, HBP2' with higher content of charge density in the two hyperbranched CPEs showed the best water solubility and the highest fluorescence quantum yield. Studies on the interactions between the three CCPs and dsDNA displayed that the electrostatic bindings of the CCPs with dsDNA/EB complex led to displacement of EB from dsDNA to the solution. HBP2' formed the most stable complex with dsDNA, and interestingly, although the charge density of HBP1' was much lower than that of LP2', HBP1' also bound to dsDNA more efficiently than LP2'. We suggested that dsDNA might enter the cavities of hyperbranched structure, and that the additional host-guest spatial interactions thereby significantly improved the binding stability of

hyperbranched CPE/dsDNA complex. Therefore, these water-soluble hyperbranched PPEs may show great potential in gene delivery and DNA biosensor applications.

Acknowledgements

The authors gratefully thank the financial support provided by the National Basic Research Program of China (Nos. 2009CB930601, 2012CB933301, 2012CB723402), the National Natural Science Foundation of China (Nos. 51073078, 21005040, 51173081, 51273092), the Natural Science Foundation of Jiangsu Province, China (BM2012010), the Science Foundation of Nanjing University of Posts and Telecommunications (NY213173), the Ministry of Education of China (No. IRT1148), the Priority Academic Program Development of Jiangsu Higher Education Institutions (PAPD) and the Synergetic Innovation Center for Organic Electronics and Information Displays.

References

[1] Thomas SW, III, Joly GD, Swager TM. Chem Rev 2007;107:1339-86.

[2] Liu B, Bazan GC. Chem Mater 2004;16:4467-76.

[3] Jiang H, Taranekar P, Reynolds JR, Schanze KS. Angew Chem Int Ed 2009;48:4300-16.

[4] Feng X, Liu L, Wang S, Zhu D. Chem Soc Rev 2010;39:2411-9.

[5] Liu X, Lan O, Cai X, Huang Y, Feng X, Fan Q, Huang W. Biosens Bioelectron 2013;41:218-24.

[6] Ho H-A, Najari A, Leclerc M. Acc Chem Res 2008;41:168-78.

[7] Huang Y-Q, Liu X-F, Fan Q-L, Wang L, Song S, Wang L-H, Huang W. Biosens Bioelectron 2009;24:2973-8.

[8] Li J, Huang Y-Q, Qin W-S, Liu X-F, Huang W. Polym Chem-UK 2011;2:1341-6.

[9] Huang Y-Q, Fan Q-L, Liu X-F, Fu N-N, Huang W. Langmuir 2010;26:19120-8.

[10] Liu X, Shi L, Hua X, Huang Y, Su S, Fan Q, Huang W. ACS Appl Mater Inter

2014;6:3406-12.

[11] Zhu C, Liu L, Yang Q, Lv F, Wang S. Chem Rev 2012;112:4687-735.

[12] Parthasarathy A, Ahn H-Y, Belfield KD, Schanze KS. ACS Appl Mater Inter 2010;2:2744-8.

[13] Chong H, Nie C, Zhu C, Yang Q, Liu L, Lv F, et al. Langmuir 2012;28:2091-8.

[14] Jiang R, Lu X, Yang M, Deng W, Fan Q, Huang W. Biomacromolecules 2013;14:3643-52.

[15] Feng X, Lv F, Liu L, Tang H, Xing C, Yang Q, et al. ACS Appl Mater Inter 2010;2:2429-35.

[16] Ding D, Li K, Zhu Z, Pu K-Y, Hu Y, Jiang X, et al. Nanoscale 2011;3:1997-2002.

[17] Liu B, Wang S, Bazan GC, Mikhailovsky A. J Am Chem Soc 2003;125:13306-7.

[18] Wu C, Bull B, Szymanski C, Christensen K, McNeill J. Acs Nano 2008;2:2415-23.

[19] Moon JH, McDaniel W, MacLean P, Hancock LE. Angew Chem Int Ed 2007;46:8223-5.

[20] Feng G, Liang J, Liu B. Macromol Rapid Commun 2013;34:705-15.

[21] Shi H, Chen X, Liu S, Xu H, An Z, Ouyang L, Huang W. ACS Appl Mater Inter 2013;5:4562-8.

[22] Bao B, Yuwen L, Zhan X, Wang L. J Polym Sci Part A Polym Chem 2010;48:3431-9.

[23] Pu K-Y, Li K, Shi J, Liu B. Chem Mater 2009;21:3816-22.

[24] Seo S, Kim D, Jang G, Kim J, Lee TS. Polymer 2013;54:1323-8.

[25] Kim YH, Webster OW. J Am Chem Soc 1990;112:4592-3.

[26] Gao C, Yan D. Prog Polym Sci 2004;29:183-275.

[27] Voit B. J Polym Sci Part A Polym Chem 2005;43:2679-99.

[28] Voit BI, Lederer A. Chem Rev 2009;109:5924-73.

[29] Xin Y, Wen GA, Zeng WJ, Zhao L, Zhu XR, Fan QL, Huang W Macromolecules 2005;38:6755-8.

[30] Mannisto M, Vanderkerken S, Toncheva V, Elomaa M, Ruponen M, Schacht E,

et al. J Controlled Release 2002;83:169-82.

[31] Reineke TM. J Polym Sci Part A Polym Chem 2006;44:6895-908.

[32] Yu M, Liu L, Wang S. J Polym Sci Part A Polym Chem 2008;46:7462-72.

[33] Wang G, Yin H, Ng JCY, Cai L, Li J, Tang BZ, et al. Polym Chem-UK 2013;4:5297-304.

[34] Bunz UHF. Chem Rev 2000;100:1605-44.

[35] Tan CY, Pinto MR, Schanze KS. Chem Commun 2002:446-7.

[36] Fan QL, Zhou Y, Lu XM, Hou XY, Huang W. Macromolecules 2005;38:2927-36.

[37] Tolosa J, Kub C, Bunz UHF. Angewandte Chemie International Edition 2009;48(25): 4610–4612.

[38] Keana JFW, Wu YX, Wu GL. J Org Chem 1987;52:2571-6.

[39] Zhou Q, Swager TM. J Am Chem Soc 1995;117:12593-602.

[40] Takahashi S, Kuroyama Y, Sonogashira K, Hagihara N. Synthesis 1980:627-30.

[41] Pu K-Y, Fang Z, Liu B. Adv. Funct. Mater. 2008;18:1321-8.

[42] Huang Y-Q, Fan Q-L, Zhang G-W, Chen Y, Lu X-M, Huang W. Polymer 2006;47:5233-8.

[43] Huang Y-Q, Fan Q-L, Lu X-M, Fang C, Liu S-J, Yu-Wen L-H, Huang W. J Polym Sci Part A Polym Chem 2006;44:5778-94.

[44] Kim DY, Choi JH, Kim SH, Cho HN, Kim CY. Synth Met 1997;84:161-2.

[45] Wang S, Bazan GC. Chem Commun 2004: 2508-9.

[46] Wang S, Liu B, Gaylord BS, Bazan GC. Adv Funct Mater 2003; 13:463-7.

[47] Birnboim HC, Jevcak JJ. Cancer Res 1981;41:1889-92.

[48] Wang S, Gaylord BS, Bazan GC. J Am Chem Soc 2004;126:5446-51.

[49] Dawn A, Nandi AK. J Phys Chem C 2007;111:6268-74.

[50] Gaylord BS, Wang S, Heeger AJ, Bazan GC. J Am Chem Soc 2001, 123, 6417-8.

Figure 1

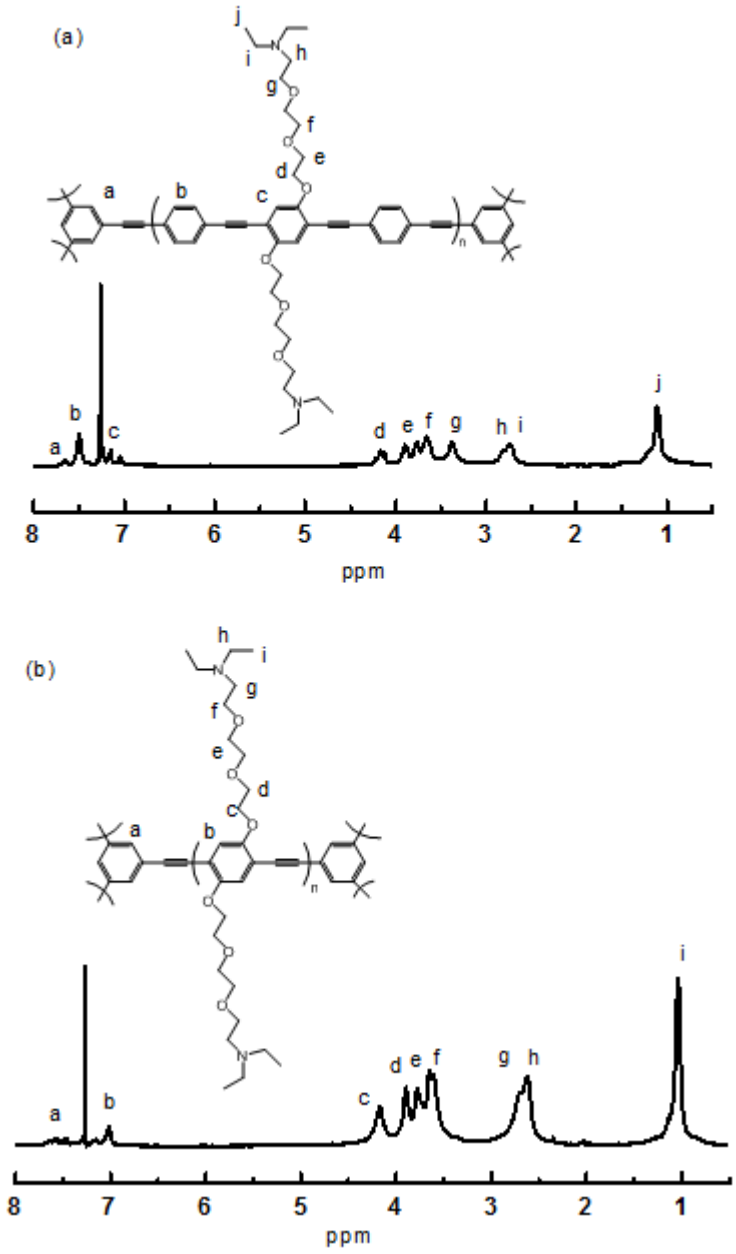

Figure 2

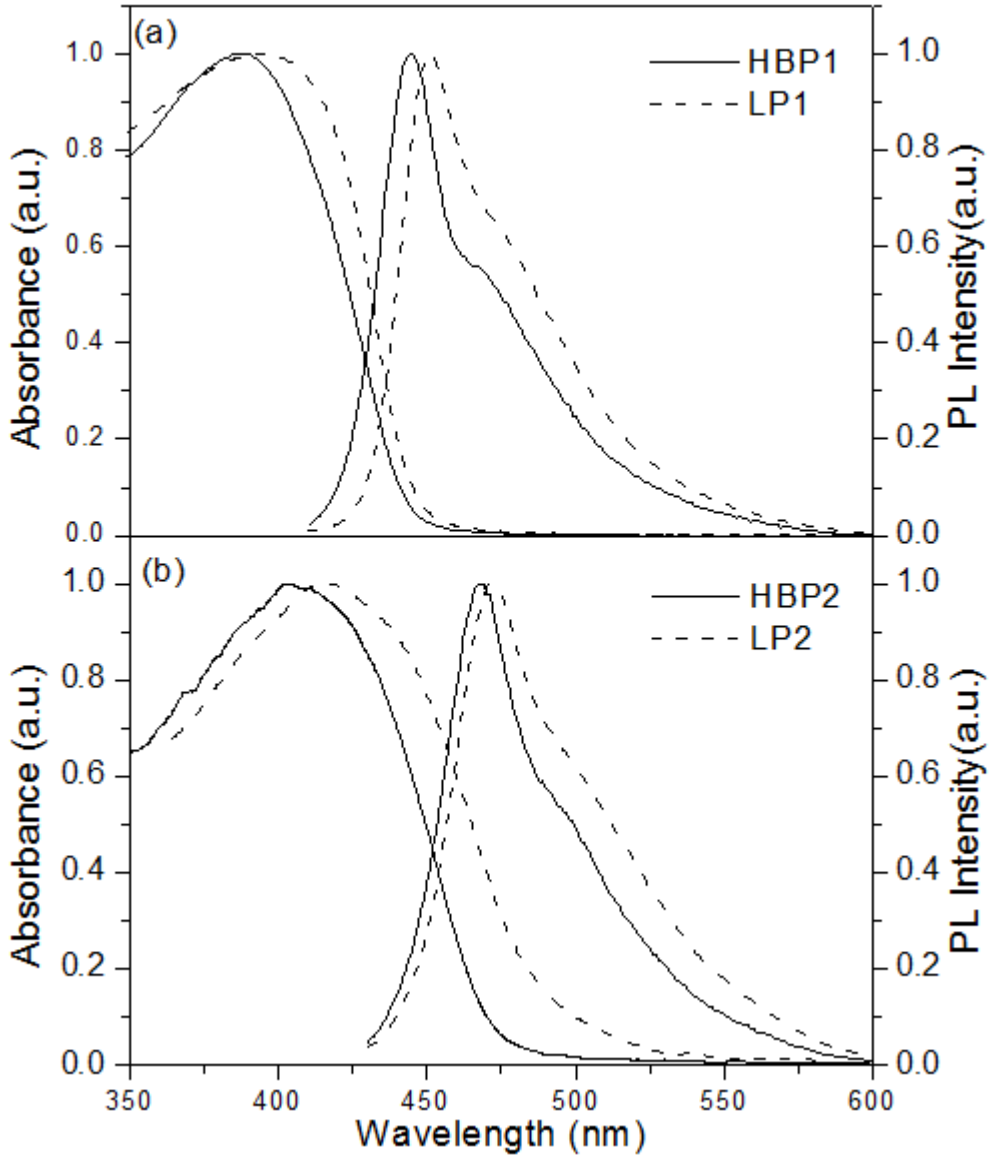

Figure 3

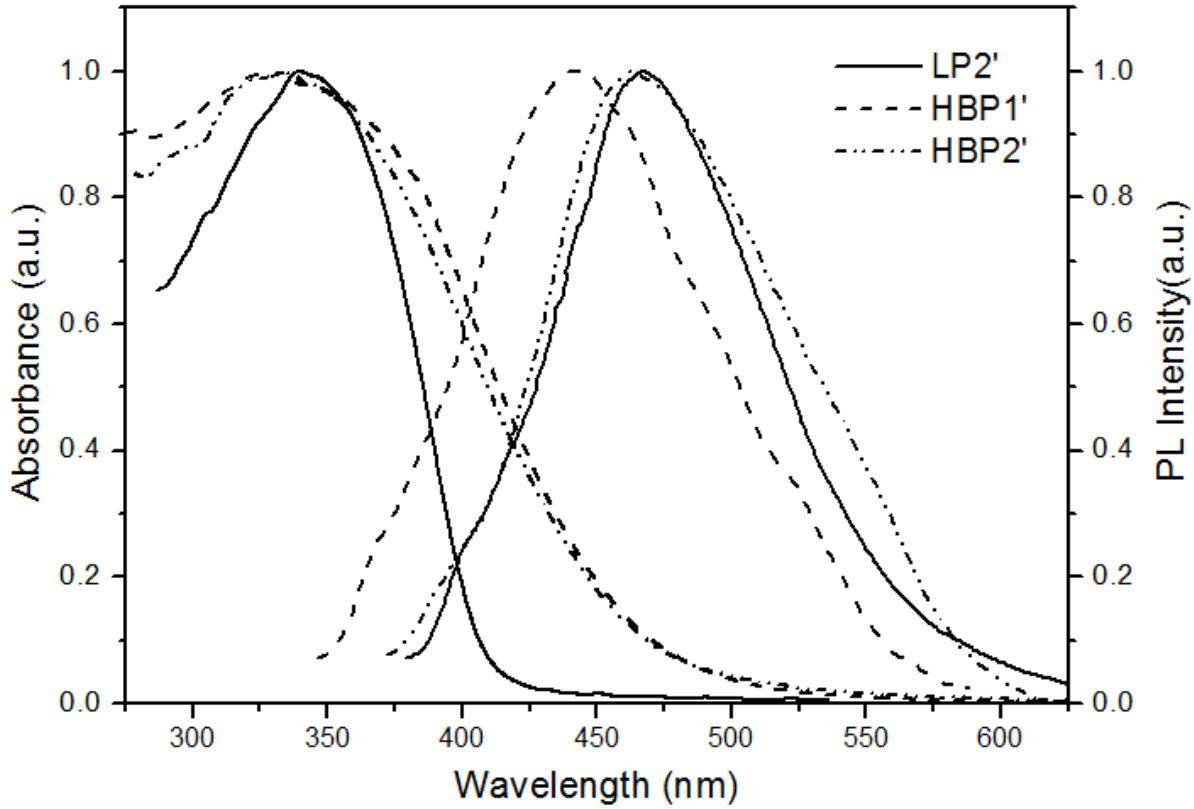

Figure 4(a)

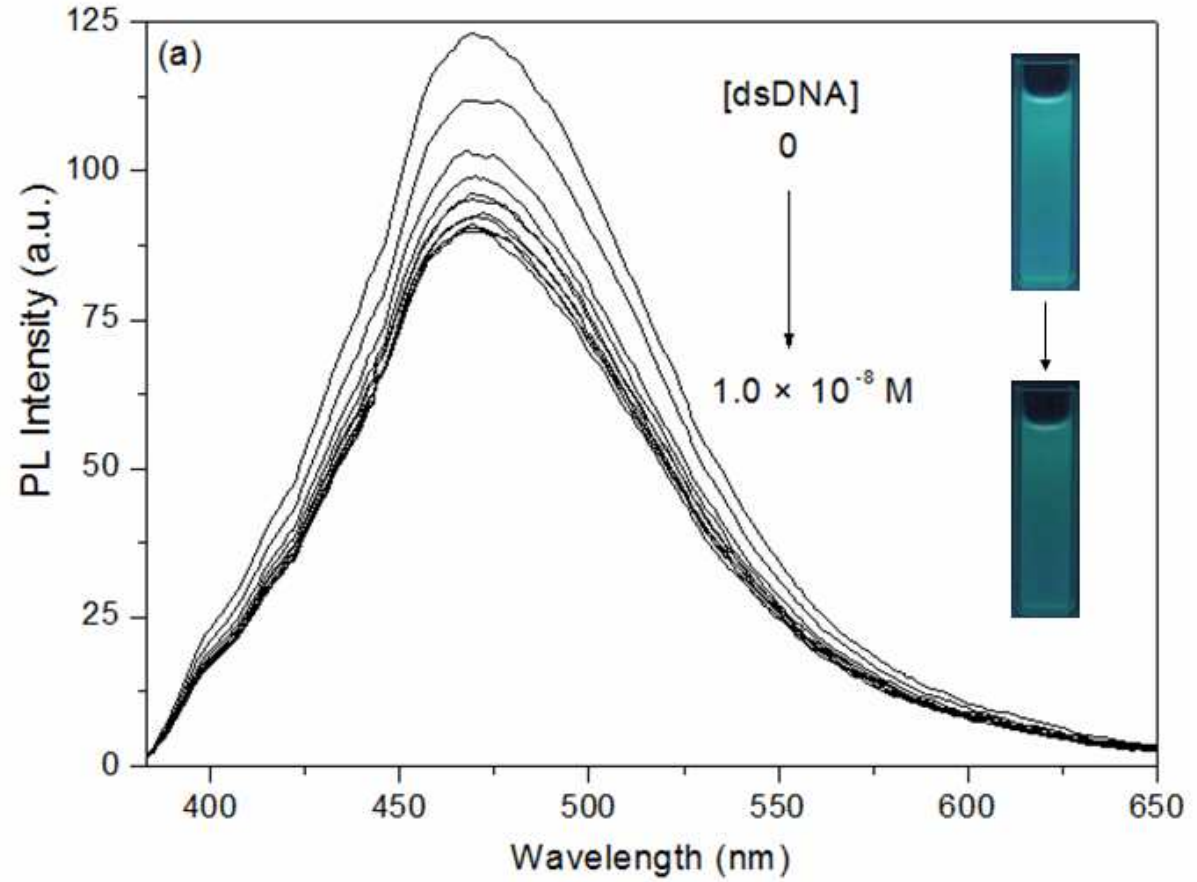

Figure 4(b)

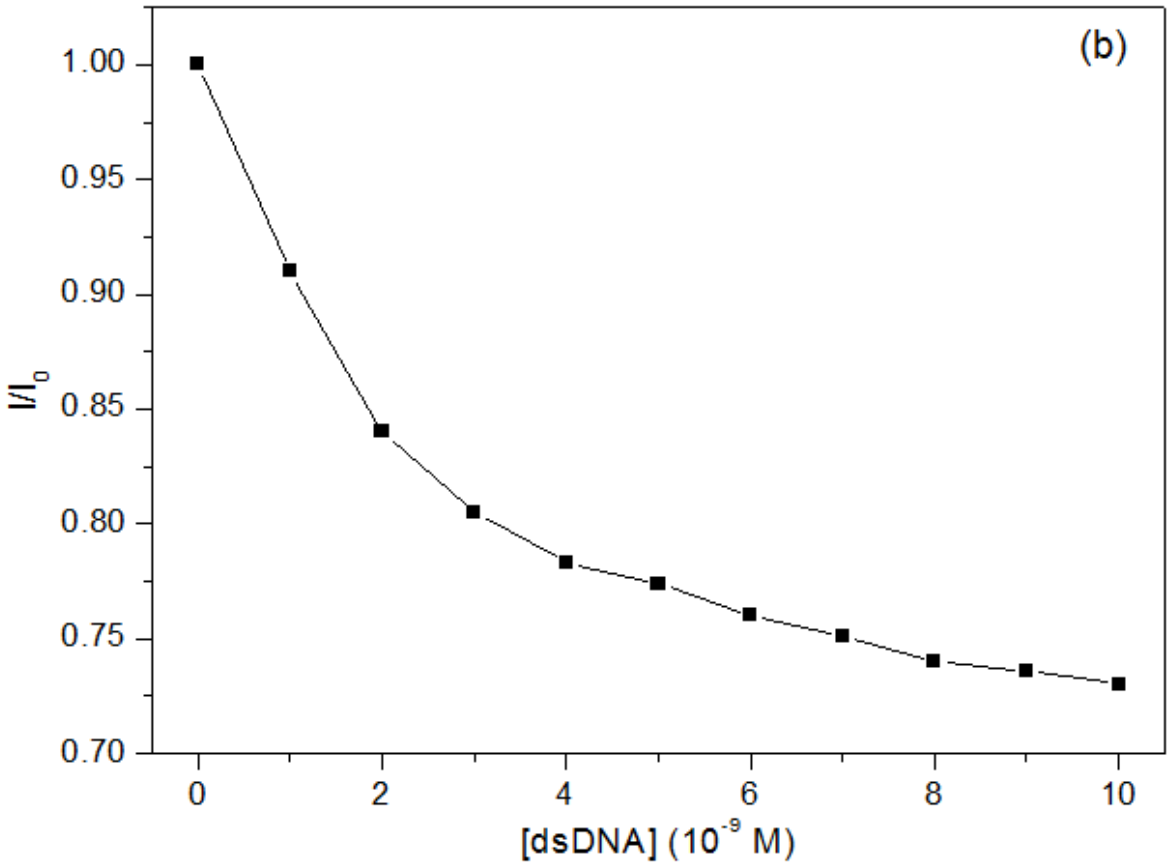

Figure 4(c)

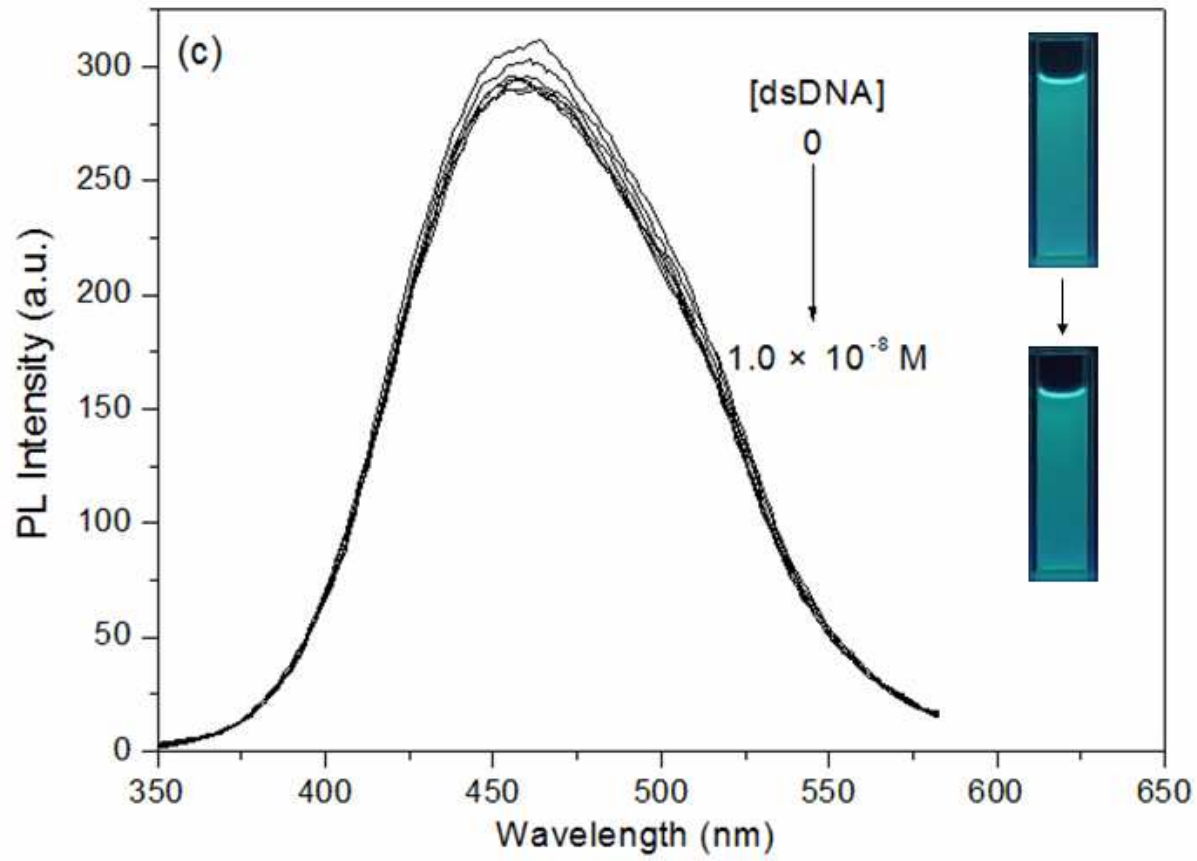

Figure 5(a)

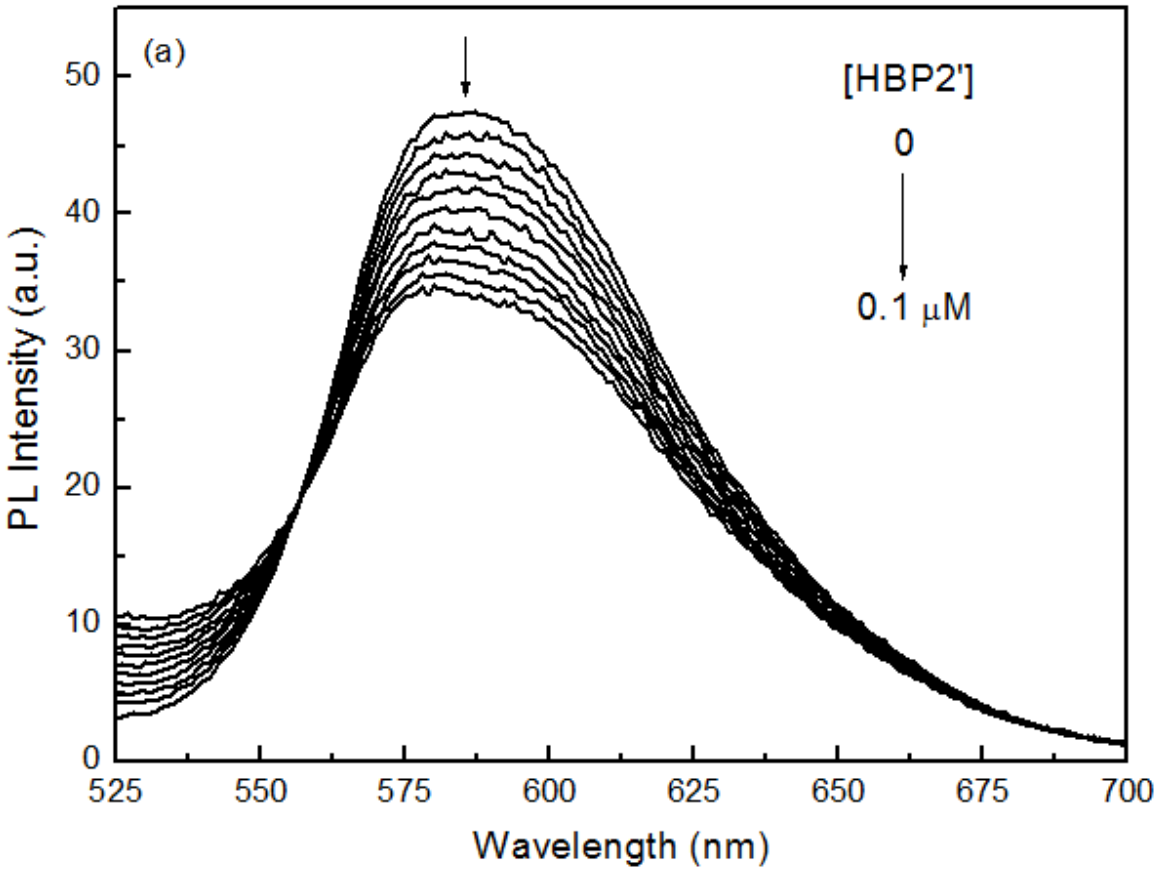

Figure 5(b)

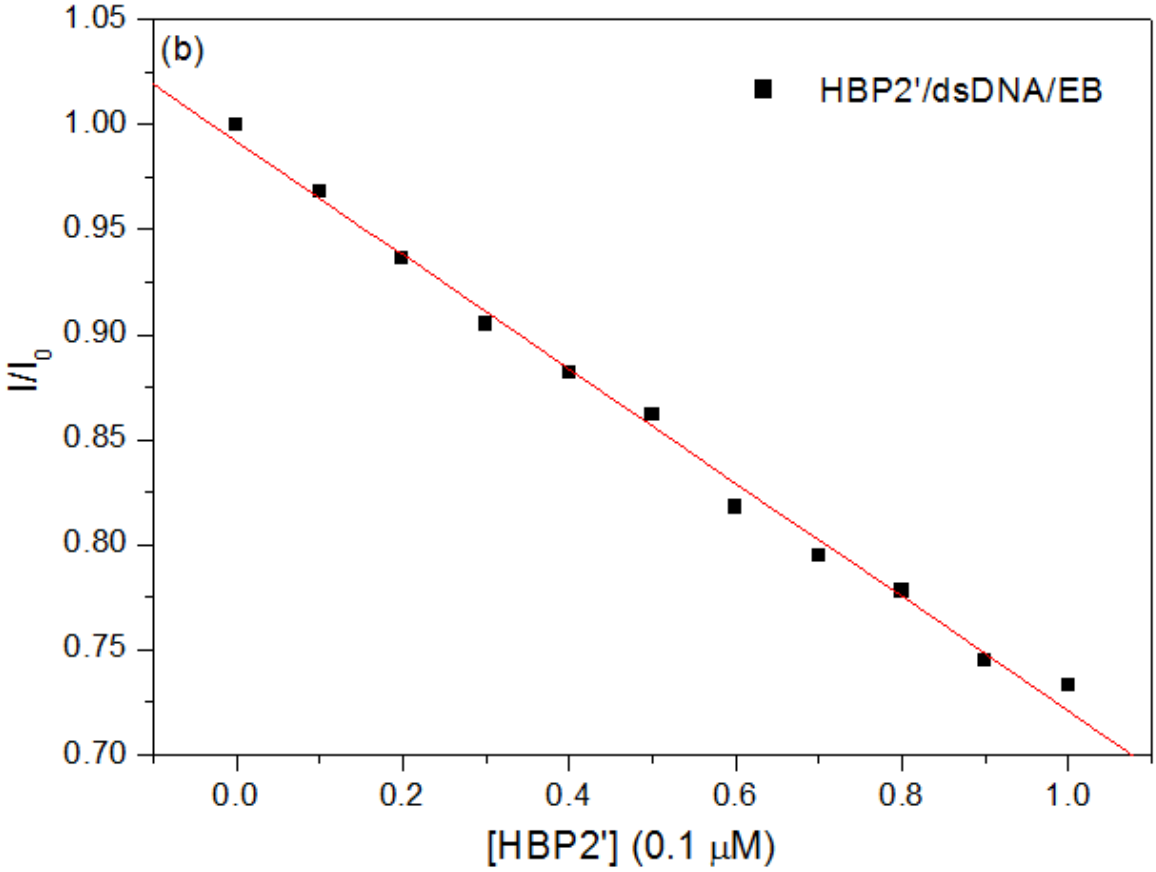

Figure 5(c)

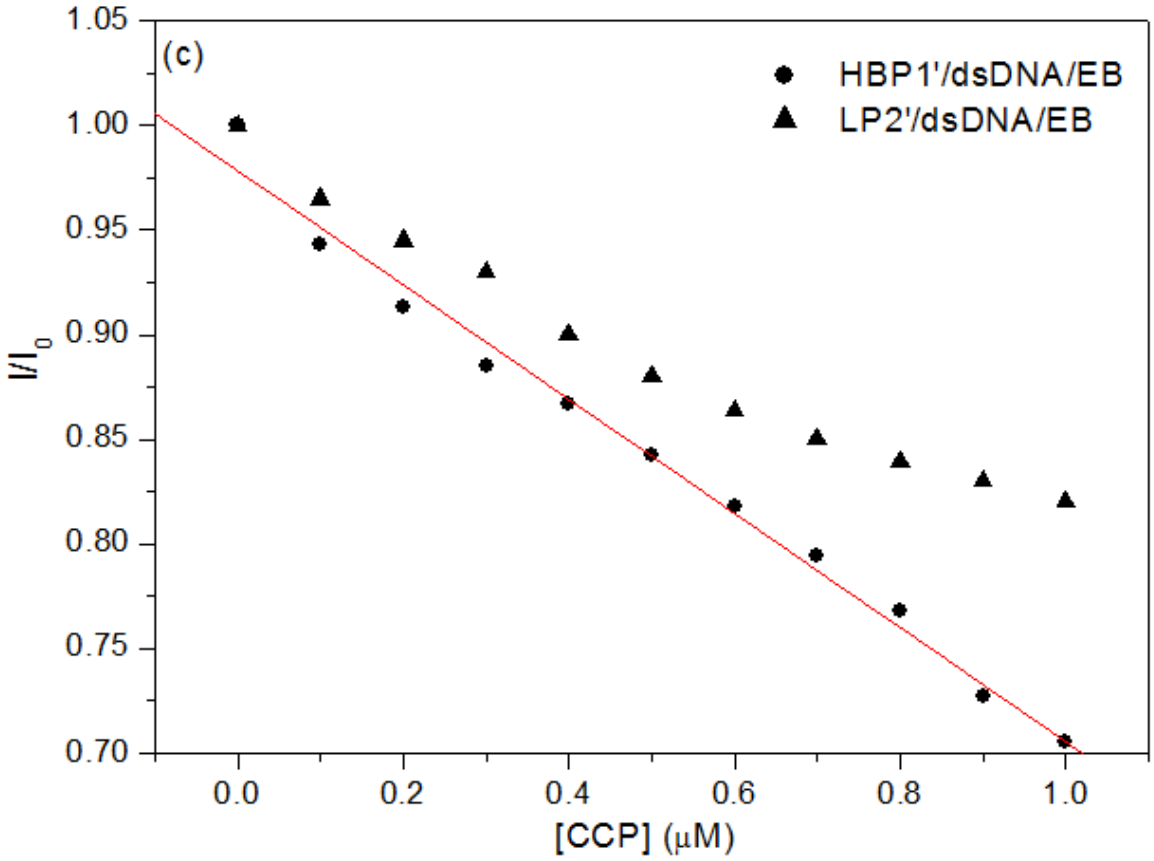

Figure 5(d)

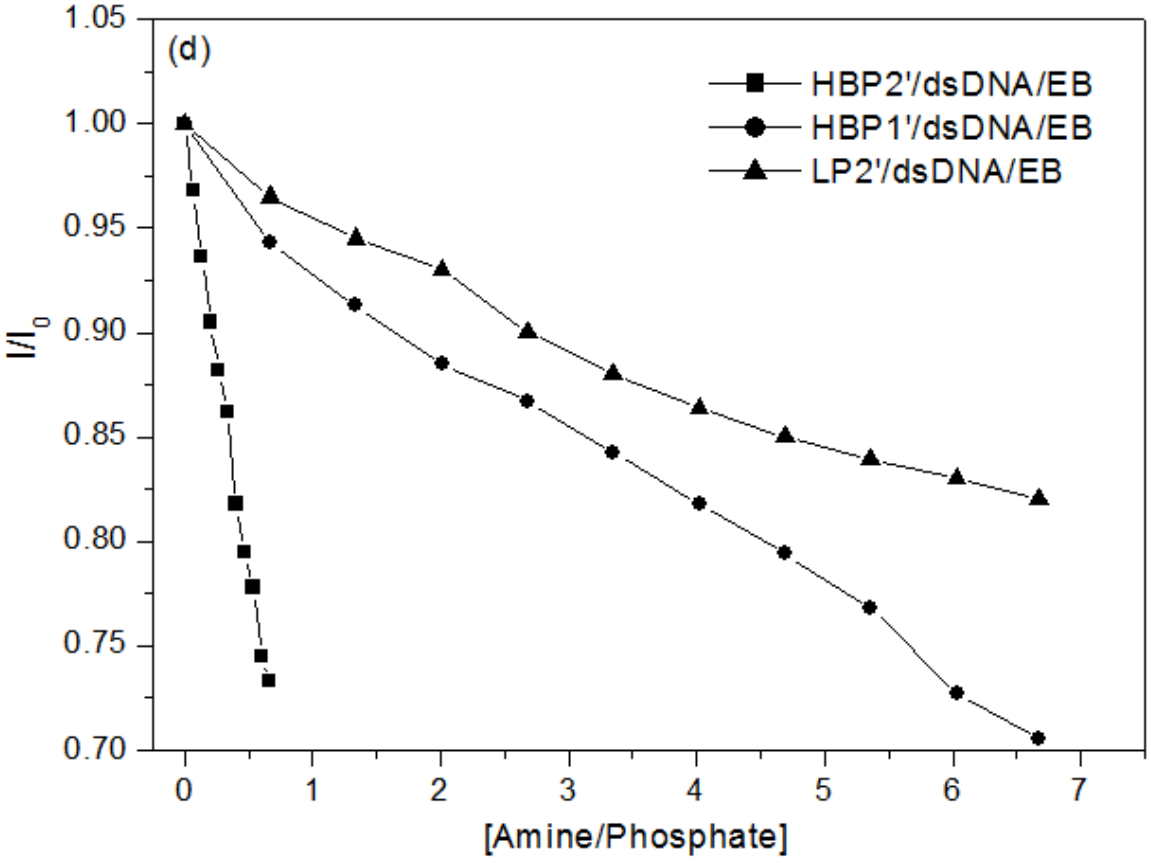

Scheme 1

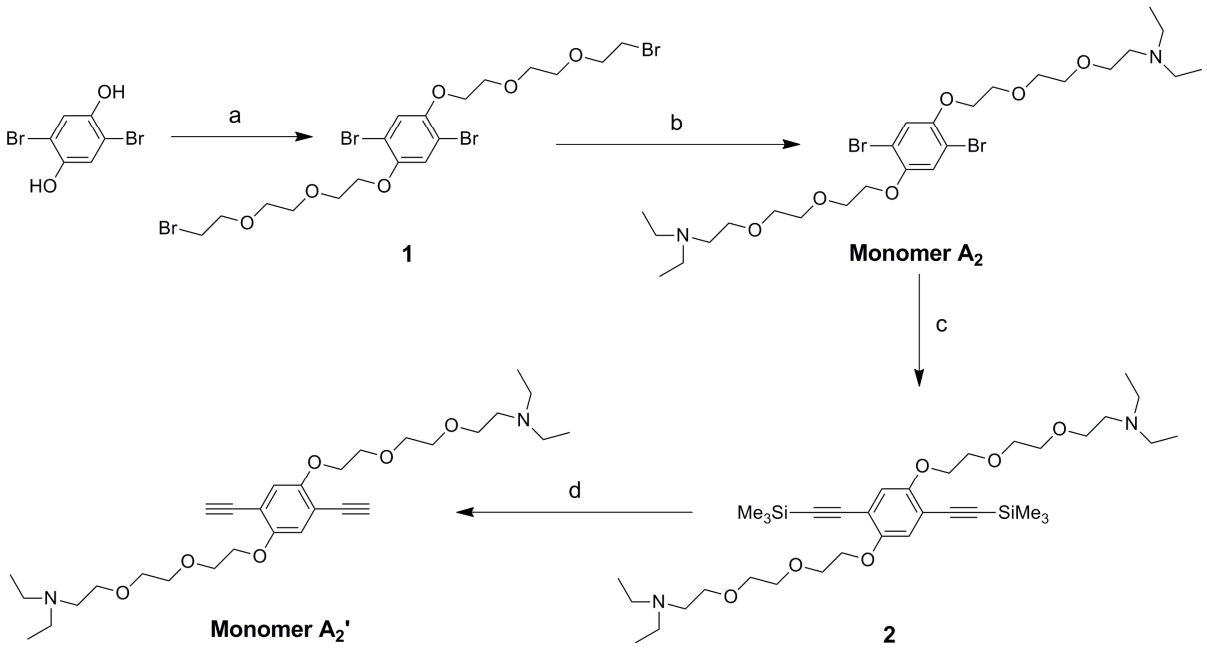

Scheme 2

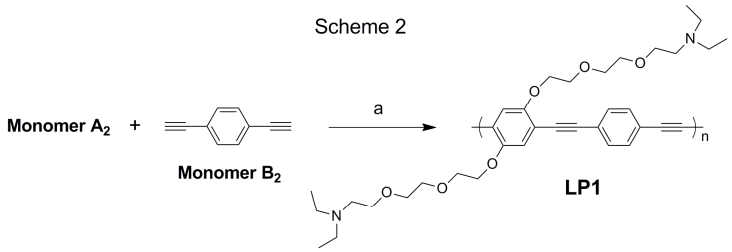

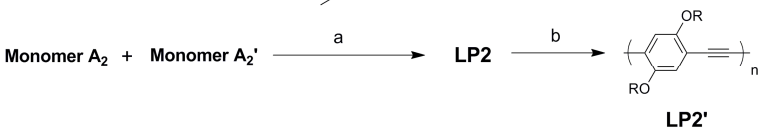

R = $CH_2CH_2OCH_2CH_2OCH_2CH_2\overset{\oplus}{N}(CH_2CH_3)_3\overset{\ominus}{Br}$

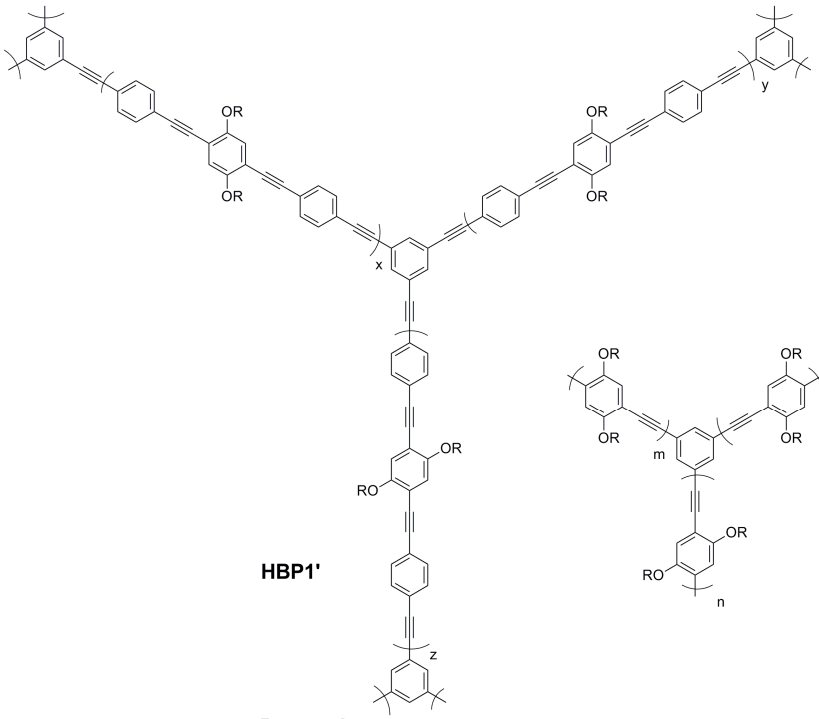

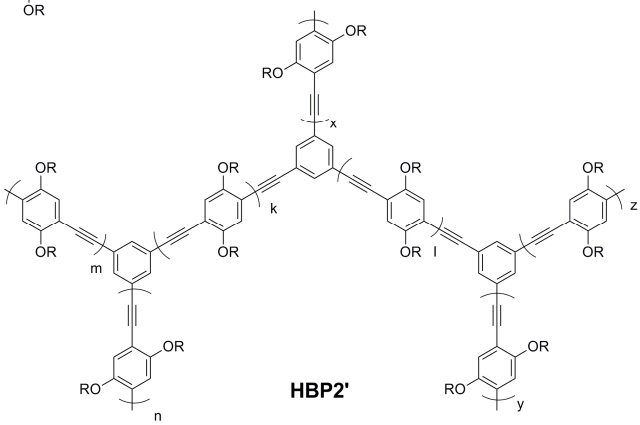

Scheme 3

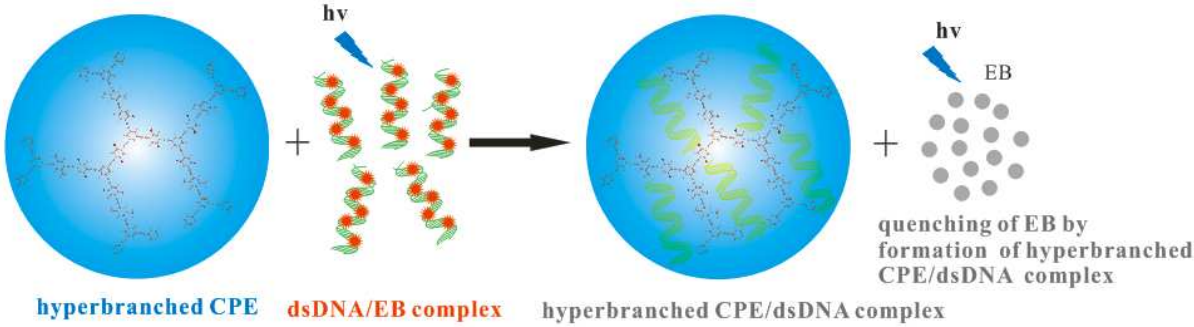

Highlights

- Two water-soluble hyperbranched poly(phenyleneethynylene)s (PPEs) with different cationic charge densities were synthesized by the simple "A_2 + B_2 (or A_2') + C_3" protocol, and their linear analogue was also synthesized for comparative investigation.
- Hyperbranched structure helped to improve water solubility and fluorescence quantum yield of conjugated polyelectrolytes.
- The hyperbranched PPE with higher cationic charge density formed the most stable complex with double-stranded DNA (dsDNA).
- DsDNA might enter the cavities of hyperbranched structures to complex with these PPEs, leading to improved binding stability.